Summer 7-15-2019

# CARBON AND NITROGEN STABLE ISOTOPES IN ORGANIC MATTER FROM LAKE CHALCO, MEXICO: A RECORD OF QUATERNARY HYDROLOGY AND CLIMATE CHANGE

Kristin Slezak Pearthree

Follow this and additional works at: https://digitalrepository.unm.edu/eps_etds

Part of the Biogeochemistry Commons

Kristin S. Pearthree
*Candidate*

Earth and Planetary Sciences
*Department*

This thesis is approved, and it is acceptable in quality and form for publication:

*Approved by the Thesis Committee:*

Peter Fawcett, Chairperson

Maya Elrick

Zachary Sharp

# CARBON AND NITROGEN STABLE ISOTOPES IN ORGANIC MATTER FROM LAKE CHALCO, MEXICO: A RECORD OF QUATERNARY HYDROLOGY AND CLIMATE CHANGE

**by**

**KRISTIN S. PEARTHREE**

B.A., Geology, Oberlin College, 2015

THESIS

Submitted in Partial Fulfillment of the
Requirements for the Degree of

**Master of Science**
**Earth and Planetary Sciences**

The University of New Mexico
Albuquerque, New Mexico

**July, 2019**

# ACKNOWLEDGEMENTS

I would like to thank many people who helped me power through this project. I would like to thank my friends and, especially, my family who listened to me talk endlessly about my research with great patience. I would like to thank my fellow graduate students for providing much humor and encouragement.

I would like to thank my collaborators on the MexiDrill project: Erik Brown, Josef Werne, Mona Stockhecke, Blas Valero Garcés, Margarita Caballero, Socorro Lozano-García, Beatriz Ortega-Guerrero, Liseth Perez, Maarten Blaauw, David McGee, Antje Schwalb, Victoria Smith, Sebastian Watt, and the MexiDrill Science Team.

I would like to thank all of the research staff in the Center for Stable Isotopes, in particular Dr. Viorel Atudorei and Dr. Laura Burkemper, for teaching me how to prepare and analyze my samples. I would also like to thank the front office staff at the University of New Mexico for answering many questions.

I would like to thank my committee members, Dr. Maya Elrick and Dr. Zachary Sharp, for their support and encouragement.

Lastly, I would like to thank my advisor, Dr. Peter Fawcett, for providing support, guidance, and encouragement through this process.

**Carbon and nitrogen stable isotopes in organic matter from Lake Chalco, Mexico:
A record of Quaternary hydrology and climate change**

**by**

**Kristin S. Pearthree**

B.A., Geology, Oberlin College, 2015
M.S., Earth and Planetary Sciences, University of New Mexico, 2019

## ABSTRACT

Sediment cores from Lake Chalco, central Mexico, were analyzed to reconstruct paleoclimate in the neotropics. This study employs total organic carbon, organic carbon-organic nitrogen ratios, carbon and nitrogen stable isotope ratios of organic matter (OM), and lithology to reconstruct changes in lake level and productivity. During Marine Isotope Stage 3 (~42-29 ka) bulk OM $\delta^{13}C$ and $\delta^{15}N$ results suggest the lake experienced strong evaporation and high pH due to warm temperatures and moderate precipitation. Large amounts of terrestrial C3 plant matter were deposited during the Last Glacial Maximum (~22-19 ka), suggesting a swampy environment resulting from reduced precipitation and cooler temperatures because the Intertropical Convergence Zone was located south of, and the mid-latitude storm track north of, Lake Chalco. The deeper part of the core records repeated changes between a lower, evaporative lake and a deeper, productive lake; sections rich in terrestrial C3 plant-rich remains may represent previous glacial maxima.

Contents

**1. Introduction**

Many aspects of past climate change in continental subtropical regions are currently poorly understood. This study examines Quaternary hydrologic change at a lake in central Mexico in order to help define natural climate variability in the subtropics. Changes in local hydrology are related to changes in regional climate, which in turn occur within the framework of global climate change. Total global insolation and distribution, determined by the orbital parameters eccentricity, precession and axis tilt, control climate cycles with longer periodicities (100 ka, 41 ka, and 23 ka). Within these longer cycles, abrupt climate change can occur during millennial-scale Dansgaard-Oeschger (D-O) and Heinrich Stadial (HS) events. Competing hypotheses suggest triggers for abrupt global climate change may lie in North Atlantic thermohaline ocean circulation or in tropical atmosphere-ocean El Niño Southern Oscillation (ENSO) interactions (Clement et al., 2001; Broecker, 2003). Paleoclimate records from the neotropics allow us to compare the timing of climate change in the subtropics to changes at higher latitudes, and to explore global teleconnection patterns that could interact during periods of rapid climate change. To better understand how anthropogenic forcing may change climate in the future, relations between tropical and global climate change require further investigation.

Cores with precise age dating collected from Lake Chalco in the Basin of Mexico provide a continuous high-resolution climate change record at a high altitude neotropical continental location that may span ~350-450 ka. The lacustrine sediment cores collected by the MexiDrill Project will help define natural variation in precipitation and

temperature at Lake Chalco through glacial-interglacial cycles, providing a better understanding of the magnitude and rates of natural climate change in the region.

Today, Mexico City has a population of over 21 million people (Kimmelman, 2017) and the basin and surrounding areas contain nearly 25% of Mexico's population. Groundwater demand is causing surface subsidence within the city, destabilizing buildings and putting stress on water resources for this population. Currently, Mexico City imports 40% of its water from distant sources (Kimmelman, 2017) and future climate change-induced drought could exacerbate this already-pressing problem. Studying paleoclimate in Central Mexico can help to refine climate models used to project possible future climate change, by defining natural climate variability in the absence of anthropogenic forcing.

## 1.1. Modern Mexican Climate

The current climate at Lake Chalco is subtropical and it is situated near the transition to the semi-arid climate in Northern Mexico. The northern extent of the temperate-tropical climates is largely controlled by seasonal variations in the position of the Intertropical Convergence Zone (ITCZ) precipitation belt and easterly trade winds that carry moisture into the region from the Gulf of Mexico and the Caribbean Sea. Because Lake Chalco is so close to this boundary, paleoclimate records can provide information on the shifting boundary between these dominant phenomena associated with global climate changes.

The mean annual temperature at Lake Chalco is ~16°C and the maximum annual temperature is ~27-28°C and occurs during late spring. The minimum annual temperature during the winter is ~4-7°C (Torres-Rodríguez et al., 2015). Mean annual precipitation is

~540 mm; most precipitation occurs from late June to September when the ITCZ is at its most northern position (Torres-Rodríguez et al., 2015). The timing of major seasonal precipitation roughly coincides with the North American Monsoon experienced farther north in Mexico and the Southwestern U.S., although the mechanisms delivering moisture are somewhat different. The remaining precipitation is associated with occasional winter storms, called *nortes*, that move into the region from the north.

Modern Central Mexico is subject to annual climate variability influenced by the extent and strength of ITCZ northward seasonal migration during the Northern Hemisphere summer, El Nino Southern Oscillation (ENSO), and occasional winter storms. This annual variability may change as a result of anthropogenic climate change; some recent modeling projections predict drying in the Mexico City area due to decreased summer precipitation (Magrin et al., 2014). The as yet uncertain response of the ITCZ to global climate change makes it more difficult to predict how climate will change in Central Mexico. Sediments obtained from the Lake Chalco core record multiple periods of substantial global climate change, and thus provide an opportunity to assess the impacts of these changes in a critical area on the northern margin of the ITCZ.



*Figure 1. Locations of long Quaternary paleoclimate records in the neotropics and subtropics. 1) Lake Chalco, Mexico 2) Cariaco Basin, Venezuela 3) Lake Peten Itza, Guatemala 4) Cave of Bells, Arizona.*

**1.2. Existing tropical climate records**

Long tropical climate records from southern North America and the Caribbean (Figure 1) have offered some opportunity to study long-term climate change in the region. These records include previous studies of

Lake Chalco sediments and other lakes in Central Mexico (Bradbury, 1971; van der

Hammen, 1974; Bradbury, 1989; Bradbury, 1997; Miranda, 1997; Metcalfe et al., 2000;

Sedov et al., 2001; Solleiro-Rebolledo et al., 2006; Roy et al., 2009; Solleiro-Rebolledo

et al., 2011; Lozano-García et al., 2015; Torres-Rodríguez et al., 2015; Holmes et al.,

2016; Ortega-Guerrero et al., 2017; Caballero-Rodríguez et al., 2018; Caballero et al.,

2019), marine sediment cores from the Cariaco Basin off of the north coast of Venezuela

(0-580 ka) (Lin et al., 1997; Peterson et al., 2000; Haug et al., 2001; Peterson and Haug,

2006; Gibson and Peterson, 2014) and cores from Lake Peten Itza in Guatemala on the

Yucatan Peninsula (0- ~400 ka) (Anselmetti et al., 2006; Hodell et al., 2008; Bush et al.,

2009; Escobar et al., 2012; Grauel et al., 2016). In addition, a speleothem record from the

Cave of Bells located in Arizona in the southwestern United States (Wagner, 2006;

Wagner et al., 2010) provides information regarding winter storm track position and

drought conditions during past glacial-interglacial cycles.

### 1.2.1. *Basin of Mexico paleoclimate*

Studies of Central Mexico Quaternary climate have historically focused on the

transition from the Last Glacial Maximum (LGM) (~ 26-19 ka; Clark et al., 2009) to the

Holocene (~11.7 ka; Cohen and Gibbard, 2016), with few records older than ~30 ka.

Some studies of paleoclimate in Central Mexico suggested the LGM was a relatively dry

period compared to the Holocene (Bradbury, 1971; Bradbury, 1989; Bradbury, 1997; Roy

et al., 2009; Solleiro-Rebolledo et al., 2011; Lozano-García et al., 2015; Holmes et al.,

2016). For a number of years, the traditional explanation for this climate pattern was a

southward displacement of the ITCZ, leading to decreased summer precipitation across

the region. However, later studies suggested that effective moisture availability during

the LGM across Central Mexico was more spatially varied than previous assumed (Metcalfe et al., 2000; Caballero-Rodríguez et al., 2018). Some studies indicate the LGM may be a wetter period (Miranda, 1997; Metcalfe et al., 2000; Sedov et al., 2001; Solleiro-Rebolledo et al., 2006; Ortega-Guerrero et al., 2017; Caballero et al., 2019). However, other records indicate the ITCZ shifted to a more southerly position during this time (Peterson et al., 2000; Haug et al., 2001; Peterson and Haug, 2006; Gibson and Peterson, 2014), so the source of moisture in central Mexico remains unclear. A possible moisture source is increased winter precipitation as a result of more winter storms penetrating further south more frequently (Bradbury, 1989; Bradbury, 1997; Correa-Metrio et al., 2012). Another possibility is that there may be a slight increase in winter precipitation, but lower mean annual temperatures and resultant lower evaporation rates are mainly responsible for increasing effective moisture across the region (Bradbury, 1989; Ortega-Guerrero et al., 2017; Caballero et al., 2019). Indeed, studies of glacial advances during the LGM on the mountains surrounding the Basin of Mexico suggest a temperature decrease of ~4-6°C (van der Hammen, 1974). Two recent papers examining pollen and diatom assemblages from an earlier Lake Chalco core suggest a mean annual temperature decrease of ~4-5°C during the LGM (Correa-Metrio et al., 2013; Caballero et al., 2019). Most studies agree that the deglacial period (~19-11.7 ka; Escobar et al., 2012; Cohen and Gibbard, 2016) was generally drier than the LGM (Metcalfe et al., 2000; Solleiro-Rebolledo et al., 2006; Roy et al., 2009; Correa-Metrio et al., 2012; Torres-Rodríguez et al., 2015; Holmes et al., 2016). Additional high resolution records spanning the time period from the LGM to the Holocene could clarify neotropical climate fluctuations associated with the transition from a glacial to an interglacial period.

Paleoclimate records in Central Mexico for time periods older than Marine Isotope Stage (MIS) 2 (~29 kya; Lisiecki and Raymo, 2005) are sparse. A few studies suggest that MIS 3/4 (71-29 kya; Lisiecki and Raymo, 2005) was a wetter period (Bradbury, 1989; Sedov et al., 2001; Solleiro-Rebolledo et al., 2011; Lozano-García et al., 2015), possibly as a result of increased Northern Hemisphere insolation driving summer precipitation. However, a study by Correa-Metrio et al. (2012) suggests Heinrich Stadials (HS) 4-5 during MIS 3, characterized by ice rafting events in the North Atlantic that cooled global climate, may have been the driest periods of the last ~50 kya, with no modern analog in the region. Some studies concluded that during MIS 3/4, Central Mexico experienced high-frequency climate oscillations with periods of high fire activity associated with severe aridity induced by increased spring insolation (Torres-Rodríguez et al., 2015; Caballero et al., 2019). These millennial-scale oscillations could be associated with HS or D-O events, but the timing of these apparent events remains unclear, so they cannot be tied to a specific HS or D-O event. The sediments from MIS 3 (57-29 kyr; Lisiecki and Raymo, 2005) remain carbonate-dominated, suggesting Lake Chalco continued to be relatively shallow and alkaline (Ortega-Guerrero et al., 2017). Low lake stands most likely associated with arid conditions persisted at Chalco during MIS 5 and even into MIS 4/3 (Ortega-Guerrero et al., 2017). A recent high-resolution study of earlier Chalco cores indicates that mid-MIS 6 (~147-130 kya), a glacial period, was relatively wet, resulting in a deep and stratified freshwater lake, as recorded by laminated diatomaceous sediments (Ortega-Guerrero et al., 2017). At the end of MIS 6 the lake became carbonate-saturated, resulting in autochthonous carbonate deposition (micritic muds), possibly due to productivity-induced high pH (Ortega-Guerrero et al.,

2017). The new record from Lake Chalco will cover 2-3 glacial terminations, but these are not as yet fully defined in the core.

The Trans-Mexican Volcanic Belt (TMVB) in Central Mexico contains many of the lakes and paleosols used in regional paleoclimate studies. This is a volcanically-active area, and volcanic activity could influence sedimentation and ecological patterns associated with climate signals in paleoclimate records. Further studies examining high-resolution records older than 30 ka could clarify competing climate and volcanism signals in lacustrine paleoclimate records from Central Mexico.

### 1.2.2. *Other North American Neotropical records*

The most widely cited Pleistocene-age record from the neotropics is from the Cariaco Basin, Venezuela. This largely-anoxic silled basin provides a record of ITCZ migration in the Caribbean for the last 580 ka. The basin traps riverine terrigenous sediment that records changes in precipitation in the watersheds of rivers draining from South America (Peterson and Haug, 2006). The results of studies examining the changes between terrigenous and biogenic sediments suggest that the ITCZ shifted its mean northern-most position south during periods of increased Northern Hemisphere cooling, stadials and glacial periods (Lin et al., 1997; Peterson et al., 2000; Haug et al., 2001; Peterson and Haug, 2006; Gibson and Peterson, 2014). This more southerly position led to drier conditions in northern South America during the LGM (Haug et al., 2001; Peterson et al., 2000; Gibson and Peterson, 2014). During periods of Northern Hemisphere warming precipitation over northern South America appears to have increased, including interstadials, interglacial periods and the early Holocene "thermal maximum" (Haug et al., 2001).

Quaternary changes in precipitation in northern South America are largely attributed to ITCZ migration patterns. The primary forcing mechanism for the ITCZ response to differential hemispheric heating remains unclear. Studies suggest both North Atlantic forcing, namely glacial meltwater input and subsequent cooling, and tropical Pacific-ENSO interactions as possible forcing mechanisms for changes in the mean annual position of the ITCZ (Haug et al., 2001; Peterson and Haug, 2006; Broccoli et al., 2006). The synchronization between the Cariaco Basin record and the Greenland ice core record indicates a strong teleconnection between the high latitudes and the tropics (Peterson and Haug, 2006). This demonstrates the necessity for research investigating ITCZ position during the Quaternary in order to better understand relations between the ITCZ and global climate change.

Lake Peten Itza, situated on the tropical Yucatan Peninsula in northern Guatemala, experiences a wet summer and dry winter due to the annual migration of the ITCZ (Anselmetti et al., 2006; Hodell et al., 2008; Bush et al., 2009). MIS 5a, MIS 4 and early MIS 3 (~85-48 ka) appear to have been relatively wet periods, with a shift towards drier conditions at ~48 ka (Hodell et al., 2008). A 2006 study by Anselmetti et al. of a core taken from Lake Peten Itza indicated that the LGM was fairly wet at this location. Further studies (Hodell et al., 2008; Bush et al., 2009) support this conclusion. This raises an important question: what climate pattern produced increased precipitation during a colder period when the Cariaco Basin record indicates the ITCZ was shifted to the south? Reduced summer precipitation but increased winter precipitation due to the deflection of the modern winter storm track south by the Laurentide Ice Sheet could have generated wetter cooler conditions (Bush et al., 2009). Pollen-based temperature reconstructions

(Correa-Metrio et al., 2012; Grauel et al., 2016) suggest humid conditions and an LGM temperature decrease of 5-10°C relative to the Holocene. The early deglacial period (~19-15 ka; Rasmussen et al., 2014) and the Younger Dryas (12.9-11.7 ka; Rasmussen et al., 2014) appear to have been the driest intervals in the last 25 ka at this location (Escobar et al., 2012). Decreased winter storm frequency, reduced summer precipitation due to the continued more southerly position of the ITCZ, and increased spring insolation are all factors thought to have contributed to drier conditions (Hodell et al., 2008; Bush et al., 2009; Escobar et al., 2012). Lake Peten Itza appears to record HS events as drier periods, likely resulting from the southerly position of the ITCZ (Bush et al., 2009; Escobar et al., 2012; Grauel et al., 2016). The early Holocene is a wetter period, likely due to a more northern mean position for the ITCZ and subsequent increased annual rainfall (Anselmetti et al. 2006; Hodell et al., 2008; Bush et al., 2009; Escobar et al., 2012).

The Cave of Bells speleothem record from southeastern Arizona, United States suggests the LGM was a period of increased precipitation at this location (Wagner, 2006). The high-resolution record spanning MIS 3-2 records millennial-scale D-O Events with periodicity of ~1500 years (Wagner, 2006). These events oscillate between cool/wet conditions during stadials and dry/warm during interstadials. Changes in atmospheric dynamics, particularly the location of the mid-latitude winter jet stream, may have increased/decreased winter precipitation across the Southwestern United States during stadials/interstadials, and increased winter precipitation during the LGM (Wagner, 2006; Wagner et al., 2010). The transition to the Holocene was stepwise, with warmer/drier conditions during the Bolling-Allerod interstadial and wetter/cooler conditions during the Younger Dryas (Wagner, 2006; Wagner et al., 2010). The record from Lake Chalco could

help constrain how far south the mid-latitude jet, and associated winter storms, extended during the LGM. Climate signals in the new Lake Chalco record can be compared to other tropical and neotropical records, such as the record from the Cave of Bells, to identify leads and lags that could indicate possible mechanisms for the changes in precipitation in the neotropics.

## 2. Site Description

Lake Chalco is one of five internally-drained lakes in the Basin of Mexico and is located just south of Mexico City (19°00'-20°00'N; 98°00'-99°30'W; 2240 m asl) in the Trans-Mexican
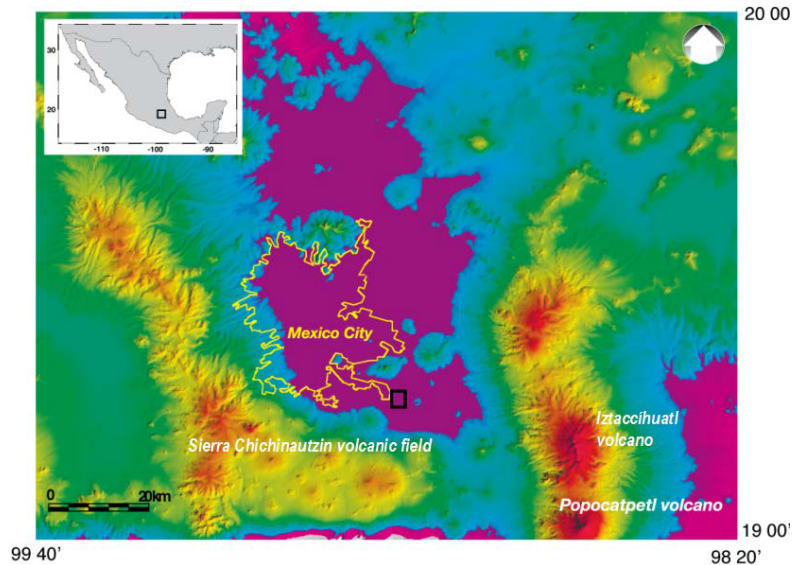


*Figure 2. Site map of the Basin of Mexico, showing the extent of the paleolake (flat magenta areas), the developed areas of the megalopolis (yellow outline), and location of coring sites in Chalco (black rectangle). Modified from Pi et al (2010).*

Volcanic Belt (Figure 2). The Trans-Mexican Volcanic Belt is an active continental arc, the result of the subduction of the Cocos Plate beneath the North American Plate (Ortega-Guerrero et al., 2017). The Basin of Mexico formed ~1.0 Ma with the eruption of the Sierra del Chichinautzin Volcanic Field (Arce et al., 2013), which closed the basin's only outlet. The five lakes, Texcoco, Chalco, Xochimilco, Zumpango, and Xaltocan, are hydrologically-linked at higher lake levels. Currently, preliminary age estimates suggest that lacustrine sediments began to collect in Lake Chalco at ~350-450 ka following basin closure, and are underlain by basalt bedrock.

Lake Chalco is located in a NNE-SSW-oriented semi-graben (Lozano-García et al., 2015) and the historical surface area of the lake was ~120 km$^2$ (Caballero and Ortega-Guerro, 1998). The lake catchment is ~1100 km$^2$ and includes the western slopes of Iztaccihuatl and Popopcatepetl volcanoes (Ortega-Guerro and Newton, 1998). The modern plant community in the Lake Chalco watershed is pine-oak forest (Rzedowski and Rzedowski, 2001). Ongoing basinal subsidence has generated a lacustrine sediment package at Lake Chalco that is ~280 m thick. Lake Chalco was drained by the Spanish and subsequent farming disrupted the upper section of the record (~0-7.55 ka). The modern remnant of the lake is an alkaline marsh with a ~1m deep water column that only exists as a result of basin subsidence due to groundwater pumping, and dries out during low precipitation years (Lozano-García et al., 1993).

Lake Chalco's location can provide information on the change in the extent of the northern migration of the ITCZ and the southward deflection of the winter storm track in response to changes in global insolation. Cores collected from Lake Chalco in 2016 through the lacustrine sequence and into the underlying basalts will be used to generate a high-resolution climate record that spans multiple glacial-interglacial cycles.

This study will examine changes in lake level, productivity, and watershed vegetation recorded by Lake Chalco sediments that are related to changes in mean annual temperature, mean annual precipitation, and seasonality of precipitation. The proxies used are total organic carbon (TOC) (%), total organic nitrogen (TN) (%), the ratio of organic carbon to organic nitrogen (C/N), and carbon and nitrogen stable isotope ratios ($\delta^{13}$C and $\delta^{15}$N) (‰) of organic matter (OM). In comparison with sediment lithology, these proxies can help identify changes in the paleo-lake environment related to changes

in regional climate over the 3-4 glacial cycles hypothesized to be present in the Chalco record.

## 3. Methods

### 3.1. Drilling, composite core, and dating

The MexiDrill Scientific Drilling Program collected three long cores and a fourth shallow core from Lake Chalco during February-April 2016. The site was identified as the lake depocenter through geophysical surveys (Figure 3). Drilling at the lake depocenter increased the likelihood of collecting the full lacustrine sequence and minimized the amount of allochthonous organic matter in the sediments, making them more useful for discerning changes in lake productivity. Staff from the Continental Scientific Drilling Coordination Office (CSDCO), the National Lacustrine Core Facility at the University of Minnesota (LacCore), and members of the MexiDrill research team facilitated the drilling, core handling, curation and field data collection (Figure 4). The International Continental Scientific Drilling Program (ICDP), the National Autonomous University of Mexico (UNAM), and the National Science Foundation (NSF) funded the drilling project. Three deep overlapping cores spanning ~280 meters of lacustrine

sediments and ~250 meters of underlying basalt, pyroclastic, and volcaniclastic deposits were collected using wireline diamond bit drilling. In addition, a short core collected sediments from the upper 20 meters of the lacustrine
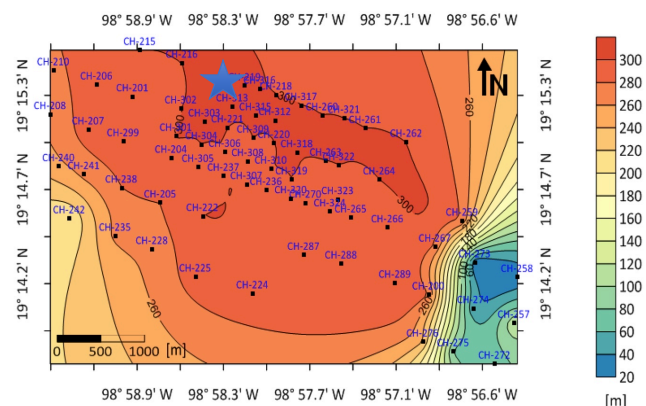


*Figure 3. Estimate of sediment thickness from passive seismic data (H/V spectra). Star denotes drilling location. Modified from Lozano-García et al., 2017.*

sequence using a Usinger coring apparatus. Core segments were split, photographed, described and stored at LacCore. Unfortunately, drilling disturbance affected 40.40 meters of the core (from 95.01 to 54.71 m) and this interval was not sampled for bulk OM chemistry. Segments from the earlier cores collected in 2008 and 2011 by researchers at UNAM will be used to fill in this section of the record.



*Figure 4. Drill rig at Lake Chalco. Photo courtesy of Peter Fawcett.*

A composite lacustrine sequence was constructed from the four cores by visually matching stratigraphy, and correlating density and magnetic susceptibility. Mona Stockhecke at the Large Lakes Observatory at the University of Minnesota Duluth and Blas Valero Garcés at the Instituto Pirenaico de Ecología completed core stratigraphy, preliminary sedimentology and composite core construction. Preliminary ^{14}C dating and age modeling for the upper section of the composite core was completed by Maarten Blaauw at Queen's University Belfast, UK, providing a numerical age chronology back to ~42 ka. There are numerous potassium-bearing tephras in the composite core, which provide the potential for multiple precise Argon-Argon (Ar-Ar) age estimates. Once the Ar-Ar dating is complete, the results for samples older than ~42 ka will be examined by age. Samples collected from the core segments were shipped to the University of New Mexico for bulk organic matter analysis.

**3.2. Sample preparation and analysis**

The individual samples here are taken from ~3 cm-long sections within the core and the average sampling interval is ~0.40 m. The samples were dried in a 70°C oven for at least 12 hours, powdered and homogenized using an agate mortar and pestle, and then dried at the same temperature for an additional 12 hours. The dry samples were then prepared for analysis.

For carbon analysis, the samples were weighed into silver capsules, with masses ranging from 2 mg to 10 mg depending on color and lithology used as estimates for total organic carbon content. The silver capsules were then fumigated with 6N Hydrochloric acid (HCl) gas for at least 12 hours. Then the samples were treated with 1-2 drops of 70°C liquid 6N HCl to remove any remaining inorganic carbon, including possible siderite ($FeCO_3$) (as per Larson et al., 2008). The samples were then left to air dry for at least 24 hours. Each capsule was then re-wrapped in a tin capsule to ensure complete combustion at a higher temperature during analysis. The samples were then analyzed using a Thermo Scientific Delta V mass spectrometer with a dual inlet and Conflo IV interface connected to a Costech 4010 elemental analyzer in the Center for Stable Isotopes at the University of New Mexico.

Carbon and nitrogen analysis was done separately because most of the samples contain significantly less nitrogen than carbon and a much larger amount of the sample was needed to record accurate $\delta^{15}N$ results. This large mass decreases the likelihood of complete inorganic carbon removal from the samples, which is necessary to analyze organic carbon chemistry. In addition, a study by Harris et al. (2001) suggested that treatment of soils by HCl fumigation to remove inorganic carbon decreased the total

nitrogen content and increased the $\delta^{15}$N value of one of their samples. A study from

Larson et al. (2008) found similar results and suggested that the shift to higher $\delta^{15}$N

values indicates that the HCl treatment releases volatile nitrogen (N$_2$) or NH$_3$+ (gas). By

analyzing carbon and nitrogen separately, the nitrogen samples are untreated, avoiding

this problem.

The amount of sample used for nitrogen analysis depended on the initial

amplitude of the nitrogen data collected with the carbon results. The amount of each

sample was then increased to the mass required to generate accurate $\delta^{15}$N results. The

samples were weighed directly into tin capsules for analysis without additional treatment.

The TOC (%) and TN (%) of each sample was calculated using a high organic

matter sediment standard with known TOC, TN, $\delta^{13}$C, and $\delta^{15}$N values relative to

international standards. The TOC and TN values were then used to calculate the C/N

ratio. The $\delta^{13}$C and $\delta^{15}$N values of each sample were calculated using the equation

$$\delta^{13}C \ or \ \delta^{15}N \ (‰) = \left(\frac{R_x}{R_{std}} - 1\right) \times 1000$$

where R$_x$ is the measured ratio of the abundance of the heavy isotope to the light isotope

of the sample and R$_{std}$ is the ratio of the abundance of the heavy isotope to the light

isotope of the standard. Here, carbon isotope ratio results are presented relative to the

international standard Vienna Pee Dee Belemnite (VPDB) and nitrogen isotope ratio

results are presented relative to the international standard AIR. The standard deviation for

isotope analyses in this study is ~±0.02‰.

## 4. Results

## 4.1. General Results

The results for the MexiDrill composite core are divided into two sections. The uppermost sediments (46.37-2.71 m) that have good numerical age constraints from radiocarbon dating and identification of known tephras are plotted by age. Deeper sediments (246.03-46.37 m) that do not currently have good age constraints are plotted by depth. In Lake Chalco, sediment types vary significantly from carbonate-rich muds to organic-rich silts and peaty material. For full lithology descriptions, see Table 1 and Table 2. Individual results for each sample are in Appendix 1. The full range of values for carbon isotope ratios of OM and C/N results are broken out by lithology (Figures 5-7) with published ranges for different organic matter sources (lacustrine algae, macrophytes, and terrestrial C3 and C4 plants). Carbon and nitrogen isotope ratios of OM results are also plotted by lithology (Figures 8-10). Results suggest lithologic facies and bulk OM results correspond well.

The banded carbonate samples consist of beds of autochthonous carbonate minerals, *Phacotus*, and ostracod shells. Some of the samples contain etched diatoms, indicating they are associated with periods of high pH. In addition, *Phacotus* only occur at pH > 8.3 (Schlegel et al., 1998) suggesting that some banded carbonate samples formed in alkaline, carbonate-saturated lake conditions. These sediments likely represent a shallower alkaline or brackish lake environment with carbonate precipitation and high biogenic productivity. The OM in the banded carbonate samples have a large range in $\delta^{13}C$ values (~ -30 to -10‰) that most likely reflects periods with higher or lower productivity and/or pH. Relatively low C/N values suggest OM in these samples is

composed of algal and macrophyte-sourced material, with little C3 plant material present (Figure 5). The $R^2$ value for the trend line from Figure 8 (not plotted) is 0.53, suggesting the carbon and nitrogen isotope ratios of OM in these samples are partially correlated. This may be the result of similar direction fractionations in both proxies at high pH, where high pH can lead to higher $\delta^{13}C$ and $\delta^{15}N$ values.

The silty clay sediments appear to represent conditions when the lake was experiencing low productivity and/or high siliciclastic deposition. These sediments consist of beds of light grey silty clay and record a lake environment dominated by fine clastic input. The TOC values of these samples are generally low (~0.20-6%), indicating clastic deposition overwhelmed organic matter deposition. This could be the result of watershed disturbance, such as high fire activity or volcanism. The relatively high $\delta^{13}C$ values (~ -20 to -11‰) for the OM of the silty clays suggest that they represent periods of low dissolved $CO_2$ in the epilimnion, possibly due to high lake pH when $HCO_3^-$ dominates dissolved inorganic carbon. Inorganic proxies such high charcoal content could indicate if these sediments are indeed the result of fire-induced watershed disturbance. The $R^2$ value for the trend line from Figure 8 (not plotted) is 0.32 and indicates the carbon and nitrogen isotope ratios of OM are not well correlated for silty clays and are likely controlled by different processes.

The sediments in the banded diatomaceous facies consist of bedded diatomaceous silty clay intercalated with siliciclastic-rich 2-5 mm thick clay beds. These sediments record a deeper lake environment dominated by diatoms and fine clastic deposition. The thin siliciclastic beds likely represent flood events transporting material from the watershed or the littoral zone into the depocenter. The banded diatomaceous samples

have an extremely wide range of both $\delta^{13}C$ values ($\sim$ -27 to -14‰) and C/N values ($\sim$5-28) (Figure 9), most likely reflecting changes in productivity within this lithologic classification and variable amounts of both macrophyte and terrestrial C3 plant material. Indeed, the $R^2$ value from Figure 9 (not plotted) is 0.01 and indicates there is no correlation between carbon and nitrogen isotope ratios of OM in these samples. Different processes are likely controlling carbon and nitrogen isotope ratios of OM in these samples.

The laminated diatomaceous sediments consist of couplets, possibly varves, of light diatomaceous bands formed by blooms during the summer and darker silty bands deposited in the winter. The couplets formed in a lake experiencing seasonal stratification and hypolimnion anoxia (Garcés, B.V. and M. Stockhecke et al., in prep.), suggesting water depths of at least 6-8 meters (Lewis, 2000). The laminated diatomaceous samples have a wide range in C/N values ($\sim$7-23), but have uniformly lower $\delta^{13}C$ values ($\sim$ -26 to -20‰). The narrow range in the carbon isotope values for these samples suggest they represent periods with similar lake conditions, when Lake Chalco was deeper, fresher, and experiencing relatively high seasonal productivity. The $R^2$ value from Figure 9 (not plotted) is 0.02 and indicates there is no correlation between carbon and nitrogen isotope ratios of OM in these samples. Different processes are likely controlling carbon and nitrogen isotope ratios of OM in these samples.
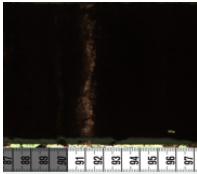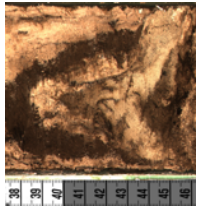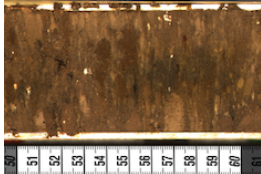
The lithology of the organic-rich samples is varied, with some samples consisting of organic-rich silty clays with sponge spicules, phytoliths, diatoms and terrestrial and amorphous aquatic matter, and some samples consisting of more peaty plant material. The peaty samples likely represent a swampy, productive environment during lake low

stands. The organic-rich sediments have a wide range of C/N values (~6-31), high TOC (18-47%), and lower $\delta^{13}C$ values (~ -23 to -28‰) (Figure 10). Some of the organic-rich silty samples may record a small eutrophic lake with higher algal productivity, producing organic-rich samples with lower C/N values (~6-15). In sharp contrast, some likely peaty organic-rich samples have much higher C/N values (~18-30), indicating more terrestrial C3 material is present. The extremely low $R^2$ value (~0) from Figure 10 (not plotted) suggest no correlation between carbon and nitrogen isotope ratios of OM in these samples. This could possibly be improved by separating the organic-rich samples into two lithologies, one corresponding to the terrestrial swamp environment, and one corresponding to the small eutrophic lake environment. Comparing the results from the C/N and carbon isotope analyses to identified macrofossils could help separate the organic-rich samples into those from a terrestrial swamp and those from a eutrophic lake environment.

**Table 1**. Lithotypes of carbonate and co-occurring sediments in the Lake Chalco core sections analyzed in this study: descriptions, depositional processes and environment. Modified from Garcés, B.V. and M. Stockhecke et al., in prep.

| Lithotype | Description | Depositional processes and environment | |
|---|---|---|---|
| **Carbonate banded (Cb)** | Decimeter-thick beds composed of autochthonous carbonate minerals (Aragonite, Calcite), ostracod shells, few diatoms with etched surfaces, minor organic remains and clastic minerals. | Shallower alkaline/brackish environment dominated by carbonate precipitation and high biogenic productivity with fine carbonate clastic input from littoral areas. |  |
| **Carbonate mottled (Cm)** | Same as Cb but with mottled silty clay clasts. | Shallower alkaline/brackish environment dominated by carbonate precipitation and high biogenic productivity. More frequent changes in lake level and higher littoral input and reworking processes. |  |
| **Carbonate massive (Co)** | Millimeter-centimeter thick laminae composed mostly of biogenic or autochthonous carbonate material. Some dominated by ostracod shells and *Phacotus*. Some are cemented if directly overlaying a v-layer. | Rapid carbonate deposition by endogenic processes (carbonate minerals) or biogenic accumulation (ostracods) in a highly productive system with limited detrital input. |  |
| **Silty Clay (Sc)** | Medium to thick beds of light grey silty clay dominated by silicate minerals with variable diatom and carbonate minerals. | Distal, deep lake environment dominated by fine clastic deposition with low bioproductivity or high clastic input due to watershed disturbance. |  |
| **Volcaniclastic (V)** | Fine ash to lapilli pumice beds. Decimeter to meter thick coarse deposits (from pebble to sand size) composed of volcanic rock fragments and volcanic material matrix. Massive, banded and with cross laminated structures. | Reworked or fallout volcanic deposits. Volcanoclastic deposits including pyroclastic flows and lahars. |  |

**Table 2**. Lithotypes of organic-rich and diatomaceous sediments in the Lake Chalco core sections analyzed in this study: descriptions, depositional processes and environment. Modified from Garcés, B.V. and M. Stockhecke et al., in prep.

| Lithotype | Description | Depositional processes and environment | |
|---|---|---|---|
| **Organic-rich (O)** | Lithotypes range from peaty to organic-rich silty clays. Organic matter includes sponge spicules, phytoliths, diatoms as well as terrestrial and amorphous aquatic organic matter. | Swamp/wetland to relatively shallow (and small) eutrophic lacustrine environment. | |
| **Diatomaceous laminated (Dl)** | Finely laminated diatomaceous silty clay with couples of light beige and dark brown laminae. Light laminae (1-2mm) contain almost only diatoms, dark laminae (2-5mm) contain more clastics. Light laminae reflect deposition during diatom blooms. Dark laminae reflect baseline deposition in the distal areas of the lake. | Relatively deep and distal fresh-water lake undergoing strong likely seasonal changes and at least partly anoxic water column. | |
| **Diatomaceous banded (Db)** | Bedded diatomaceous silty clay intercalated often by grey siliciclastic-rich 2-5 mm thin clay beds. | Distal, deep lake environment dominated by fine clastic and diatom deposition. Grey layers deposited during flood events transporting material from littoral areas and/or watershed. | |
| **Diatomaceous mottled (Dm)** | Diatom-rich clayey silt with speckle of beige diatom clasts in a relatively homogenous matrix. | Distal but shallower environment with redox fluctuations responsible for mottling textures. | |
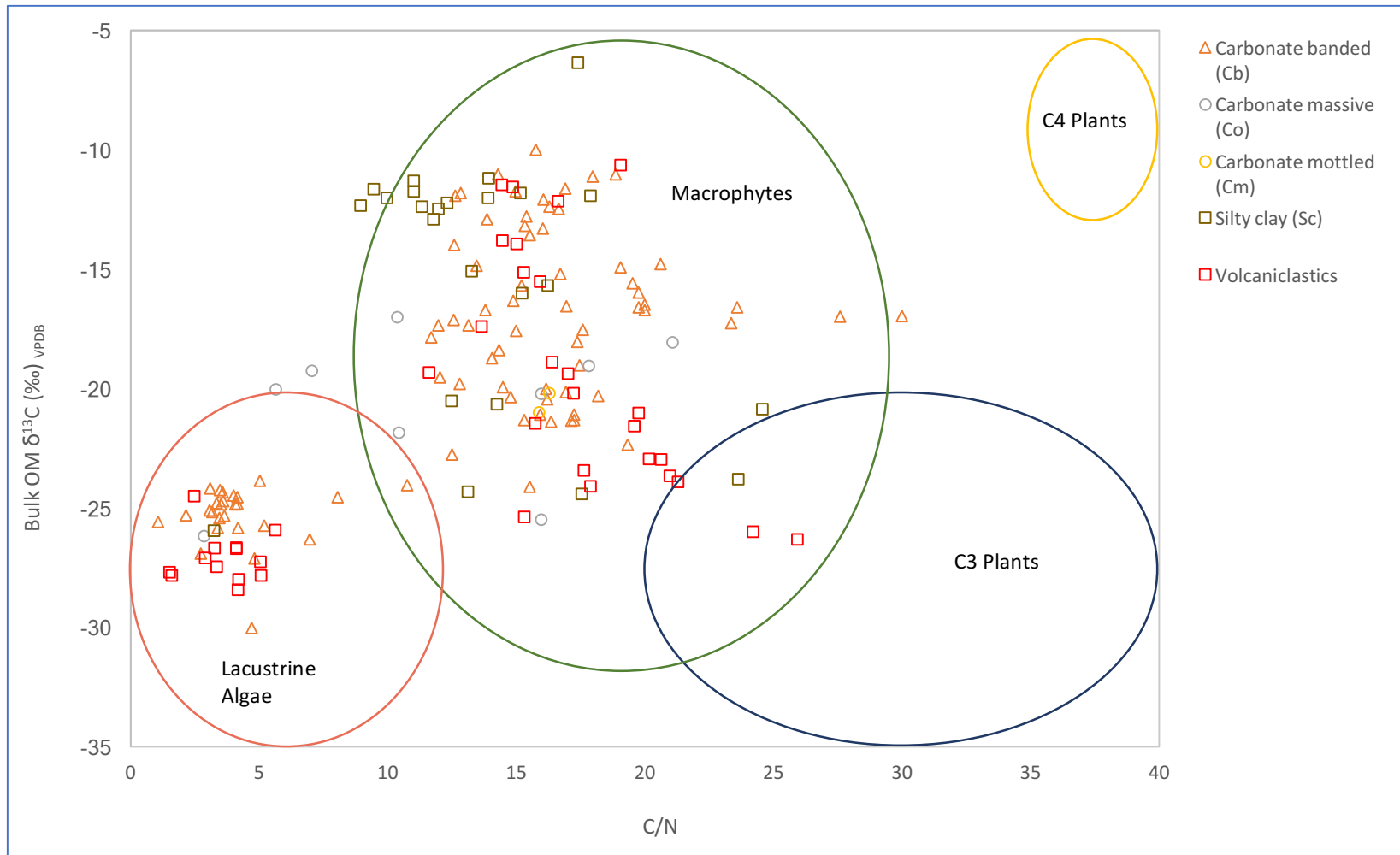
Figure 5. $\delta^{13}C$ values and C/N ratios of organic matter indicate sources of OM in Lake Chalco carbonate, silty clay, and volcaniclastic sediments. The ranges of $\delta^{13}C$ and C/N values for potential OM sources are from Keely and Sandquist, 1992; Talbot and Johannessen, 1992; Meyers and Ishiwatari, 1993; Meyers, 1994; Meyers and Lallier-Vergès, 1999; Abbott et al., 2000; Talbot and Lærdal, 2000; Filley et al., 2001; Dawson et al., 2002; Leng and Marshall, 2004; Aichner et al., 2010; Kohn, 2010.
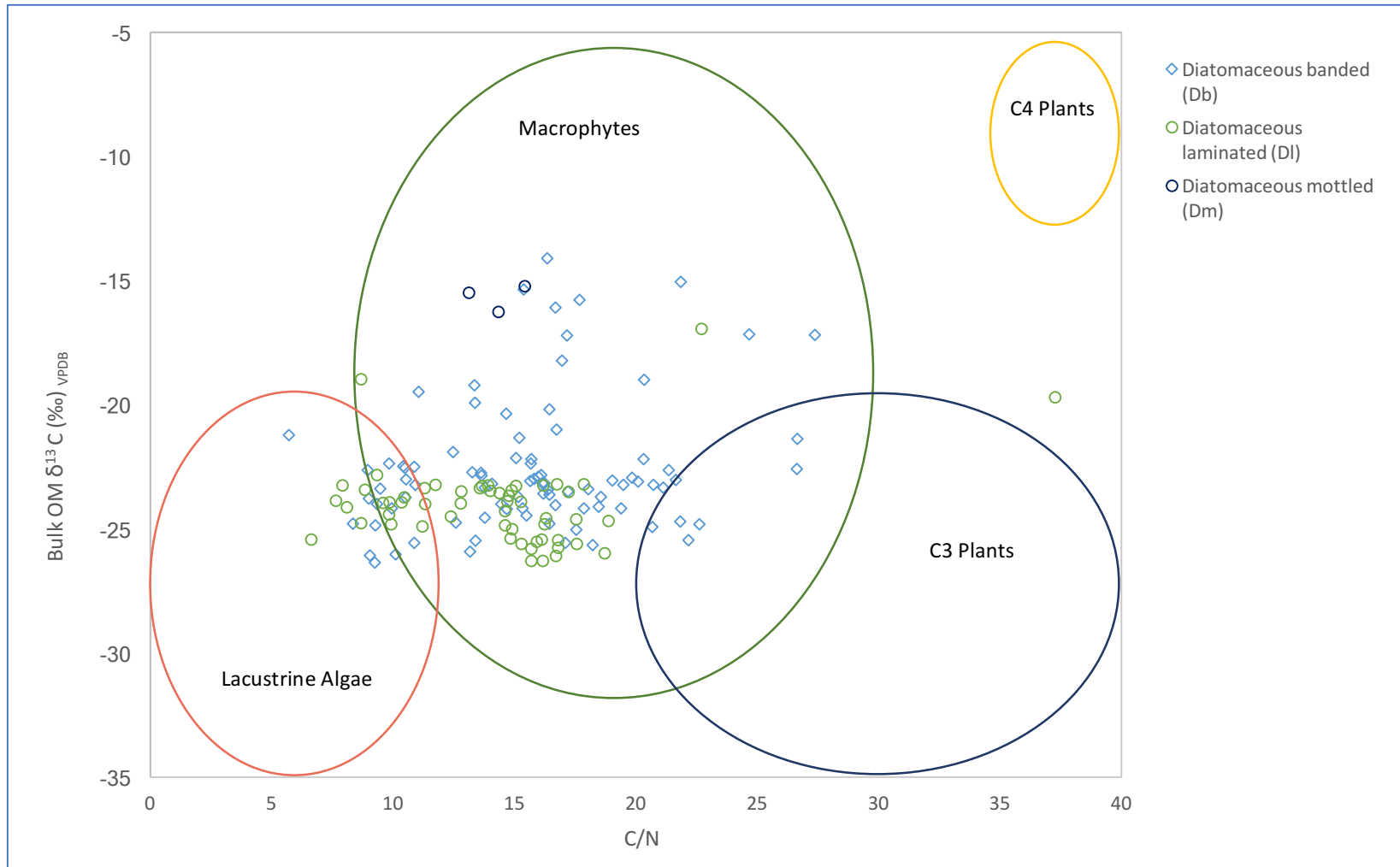
*Figure 6. δ¹³C values and C/N ratios of organic matter indicate sources of OM in Lake Chalco diatomaceous sediments. The ranges of δ¹³C and C/N values for potential OM sources are from Keely and Sandquist, 1992; Talbot and Johannessen, 1992; Meyers and Ishiwatari, 1993; Meyers, 1994; Meyers and Lallier-Vergès, 1999; Abbott et al., 2000; Talbot and Lærdal, 2000; Filley et al., 2001; Dawson et al., 2002; Leng and Marshall, 2004; Aichner et al., 2010; Kohn, 2010.*

*Figure 7. $\delta^{13}C$ values and C/N ratios of organic matter indicate sources of OM in Lake Chalco organic-rich sediments and sediments disturbed by drilling. The ranges of $\delta^{13}C$ and C/N values for potential OM sources are from Keely and Sandquist, 1992; Talbot and Johannessen, 1992; Meyers and Ishiwatari, 1993; Meyers, 1994; Meyers and Lallier-Vergès, 1999; Abbott et al., 2000; Talbot and Lærdal, 2000; Filley et al., 2001; Dawson et al., 2002; Leng and Marshall, 2004; Aichner et al., 2010; Kohn, 2010.*
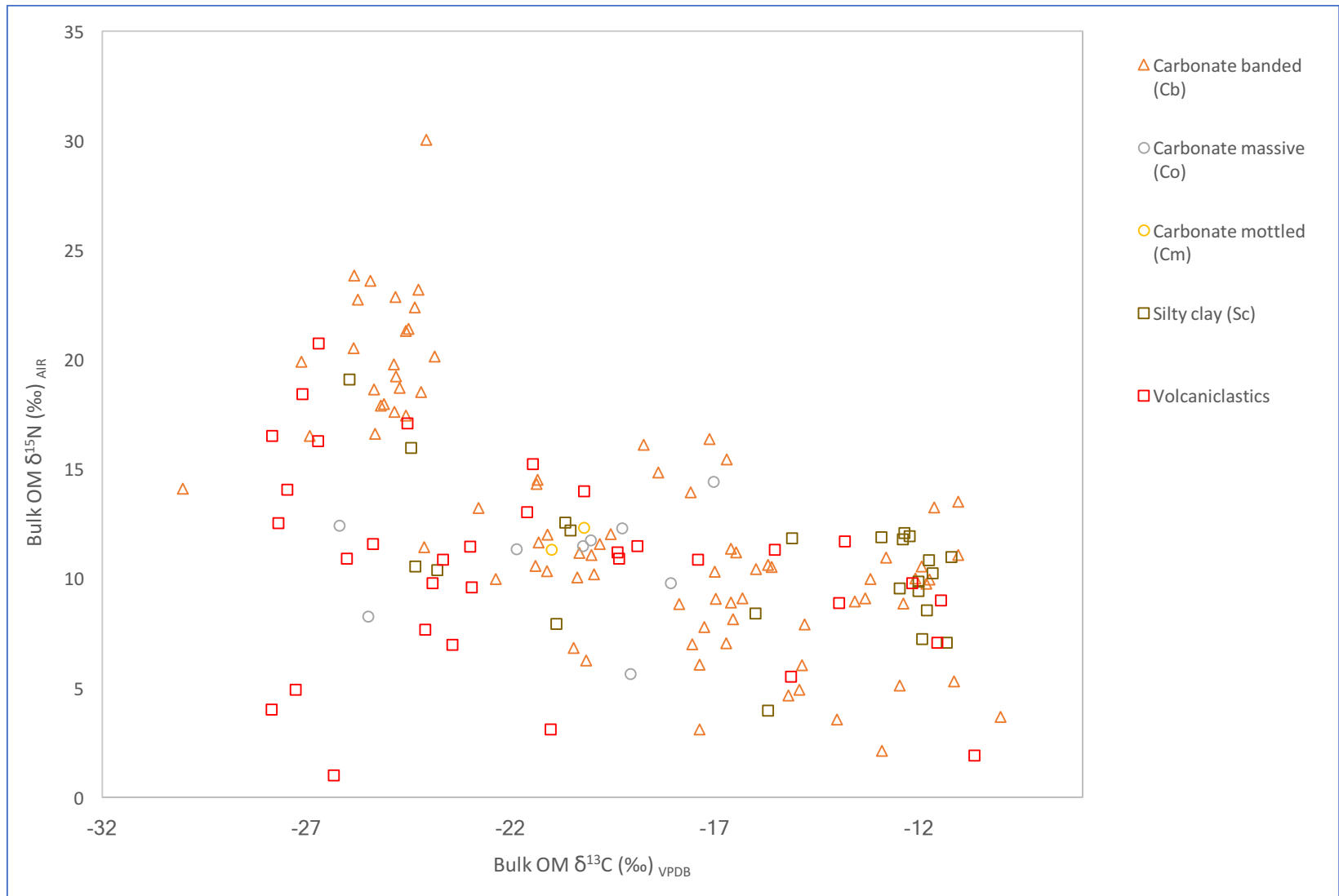
*Figure 8. Carbon and nitrogen isotope ratios of OM in Lake Chalco carbonate, silty clay, and volcaniclastic sediments. $R^2$ values for linear trend lines (not shown) for each sample type are: banded carbonates $R^2$=0.53, massive carbonates $R^2$=0.02, silty clays $R^2$=0.32.*
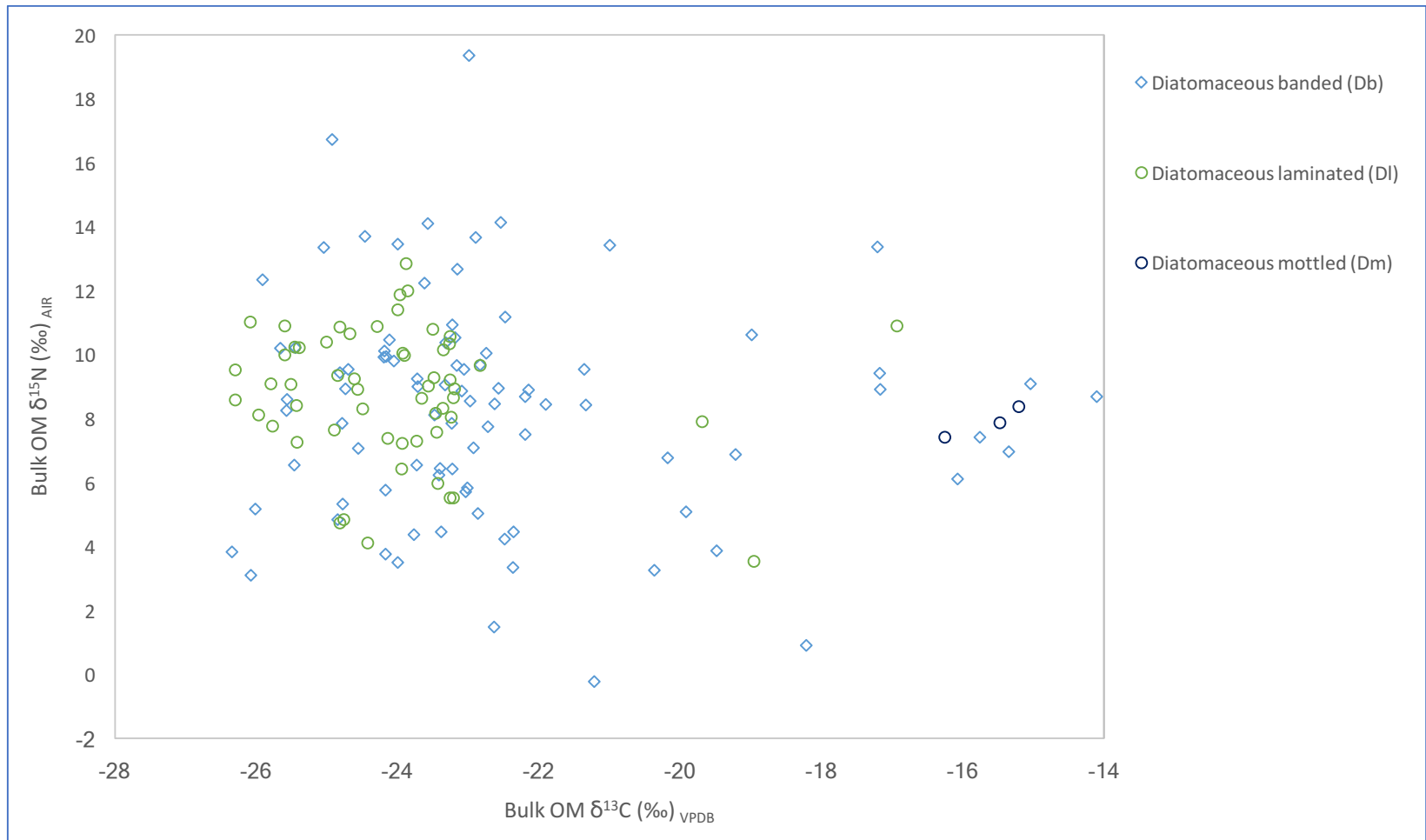
Figure 9. Carbon and nitrogen isotope ratios of OM in Lake Chalco diatomaceous sediments. $R^2$ values for linear trend lines (not shown) for each sample type are: laminated diatomaceous $R^2=0.02$, banded diatomaceous $R^2=0.01$.
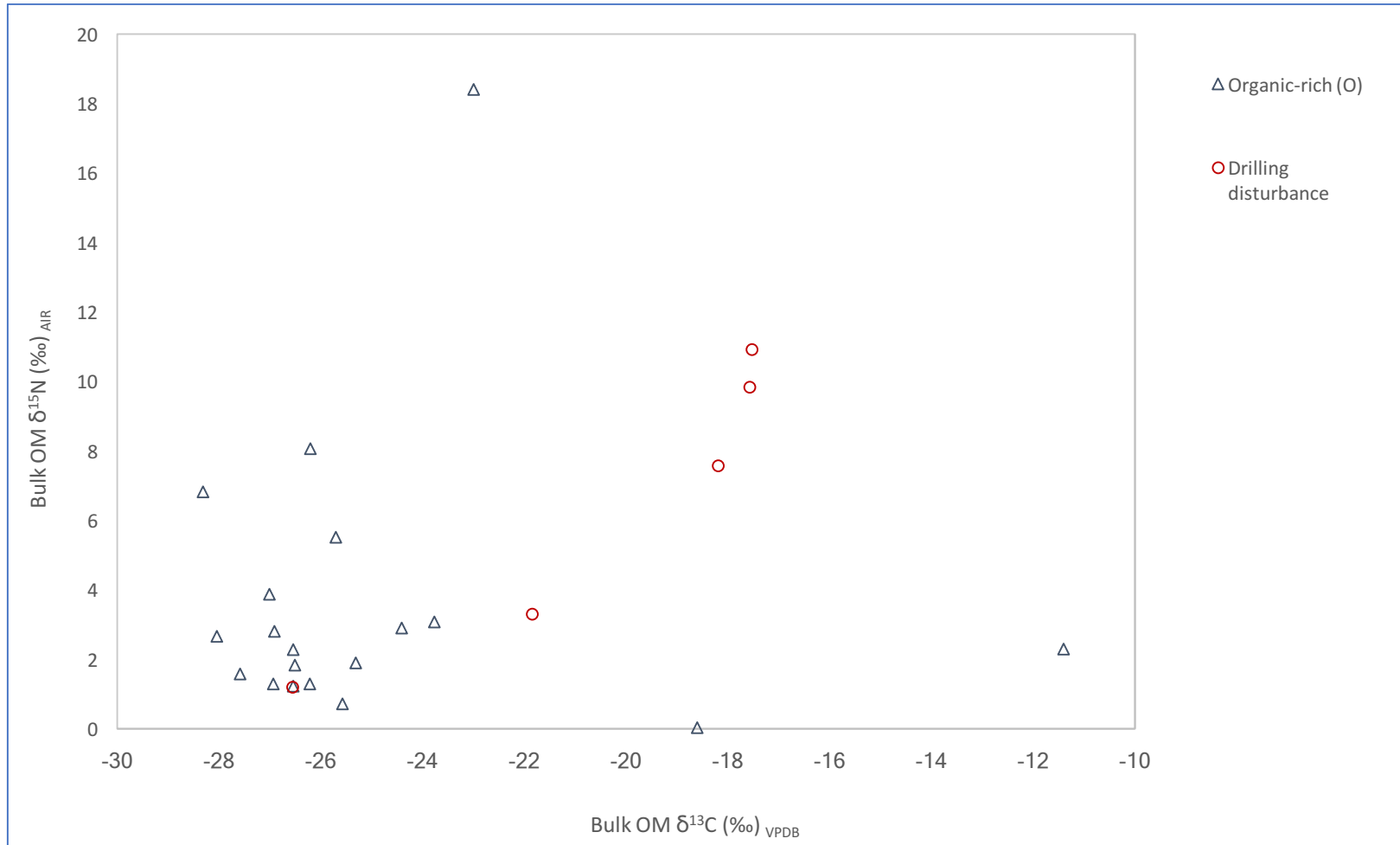
*Figure 10. Carbon and nitrogen isotope ratios of OM in Lake Chalco organic-rich sediments and sediments disturbed by drilling. $R^2$ values for linear trend lines (not shown) for the organic-rich samples is $R^2$=6.8E-05 (≈0).*
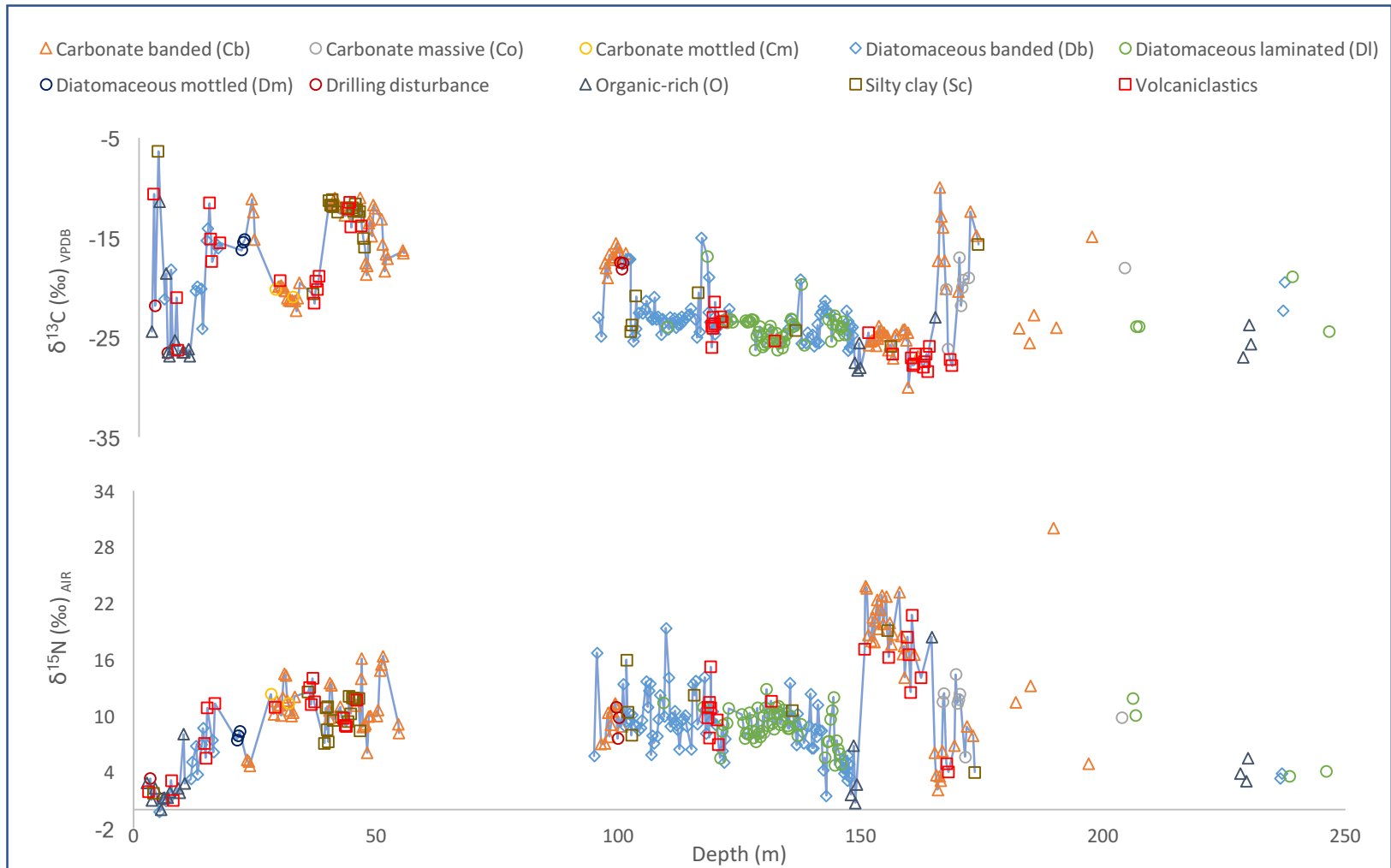
*Figure 11. Carbon and nitrogen isotope ratios of OM in Lake Chalco sediments from the entire composite core (246.03-2.71 m depth).*
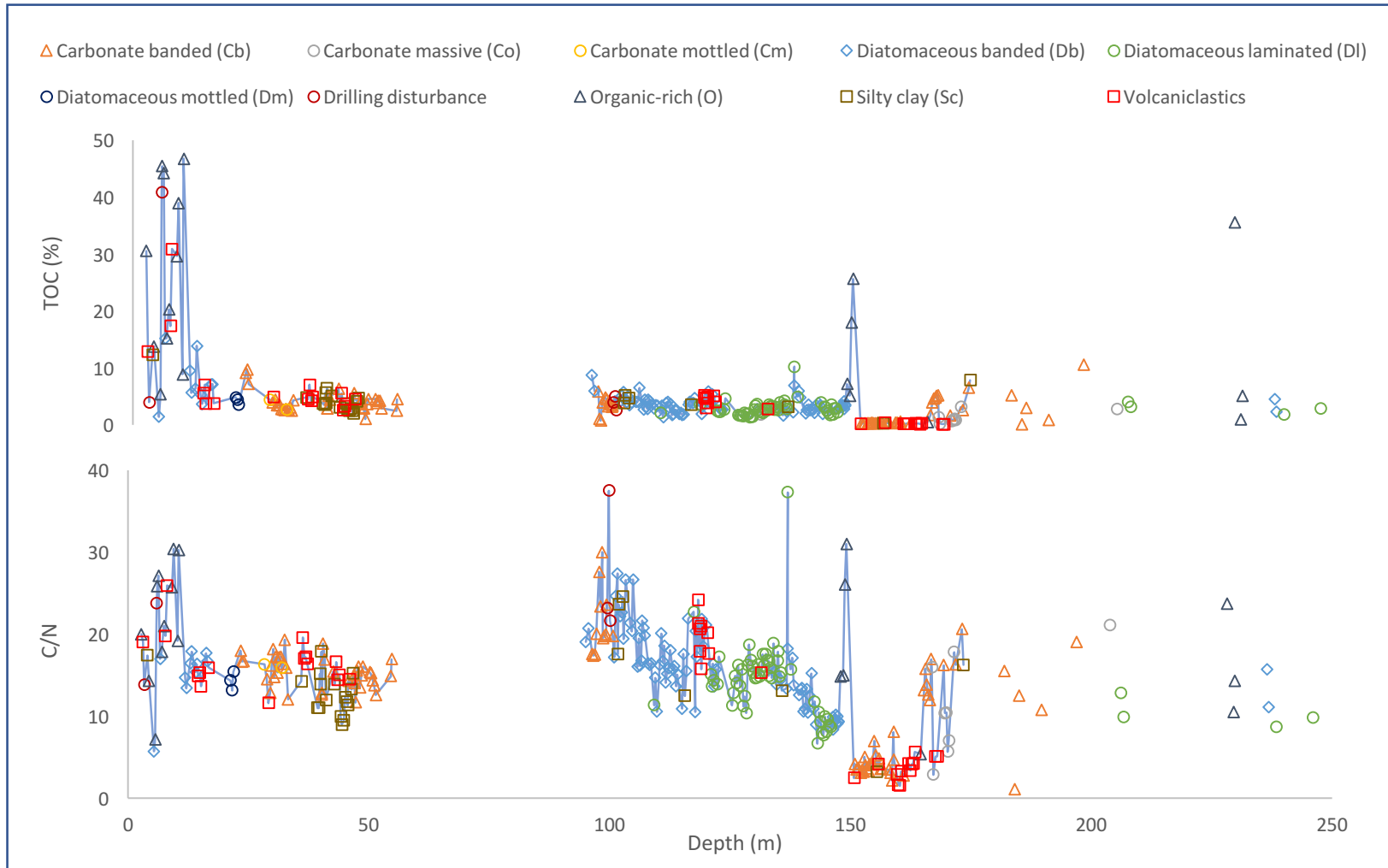
*Figure 12. TOC and C/N results from Lake Chalco organic matter for the entire composite core (246.03-2.71 m depth).*

## 4.2. Results for radiocarbon-dated section (~42-7.5 ka; 46.37-2.71 meters)
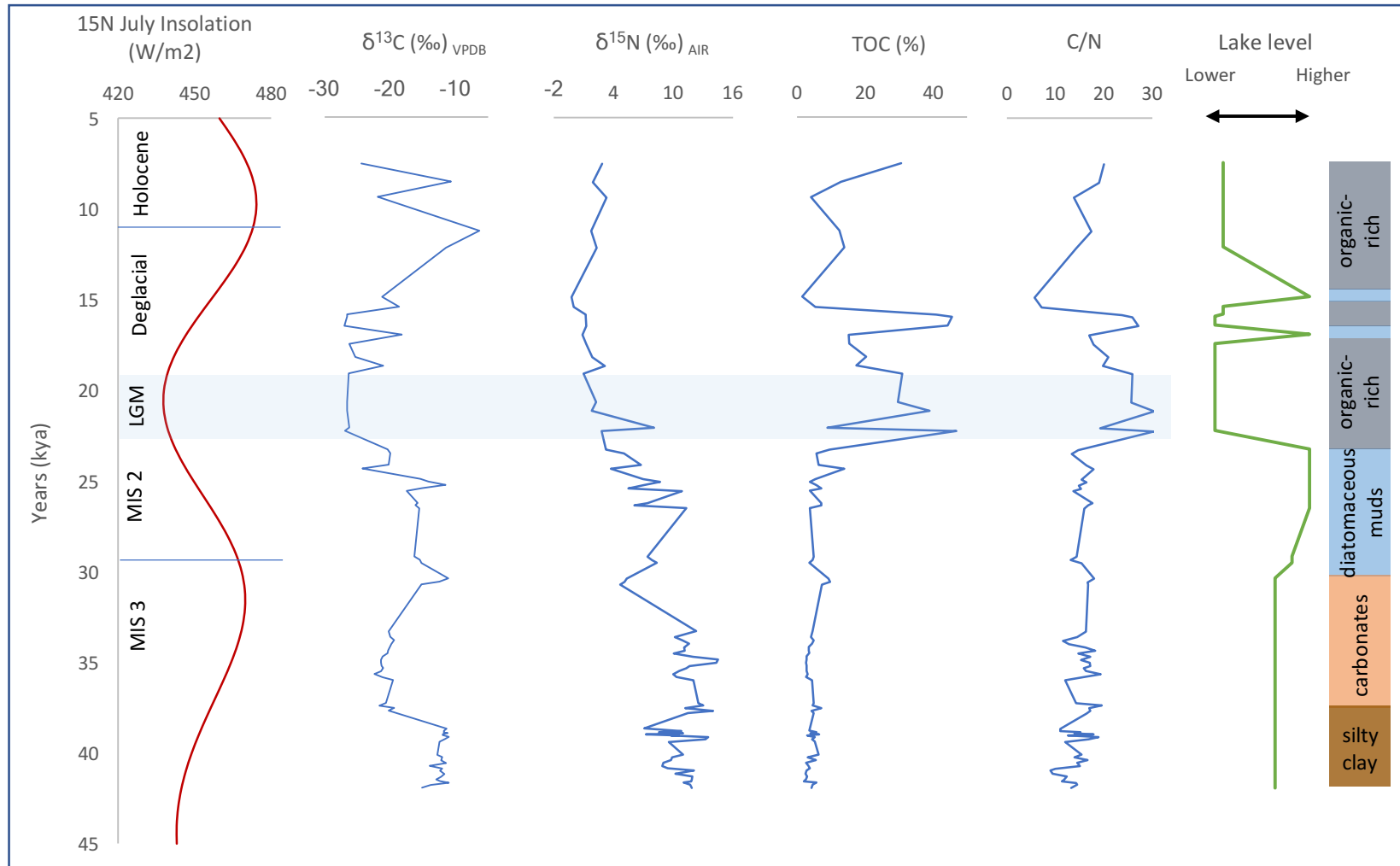


*Figure 13. Carbon and nitrogen isotope ratios of OM, TOC, C/N, stratigraphy, and interpretation of relative changes in lake water level for the radiocarbon-dated section of the core (41.91-7.55 kya; 46.37-2.71m). Insolation data are from Berger, 1992.*

## 4.3. Results with depth (246.03 - 46.37 m)
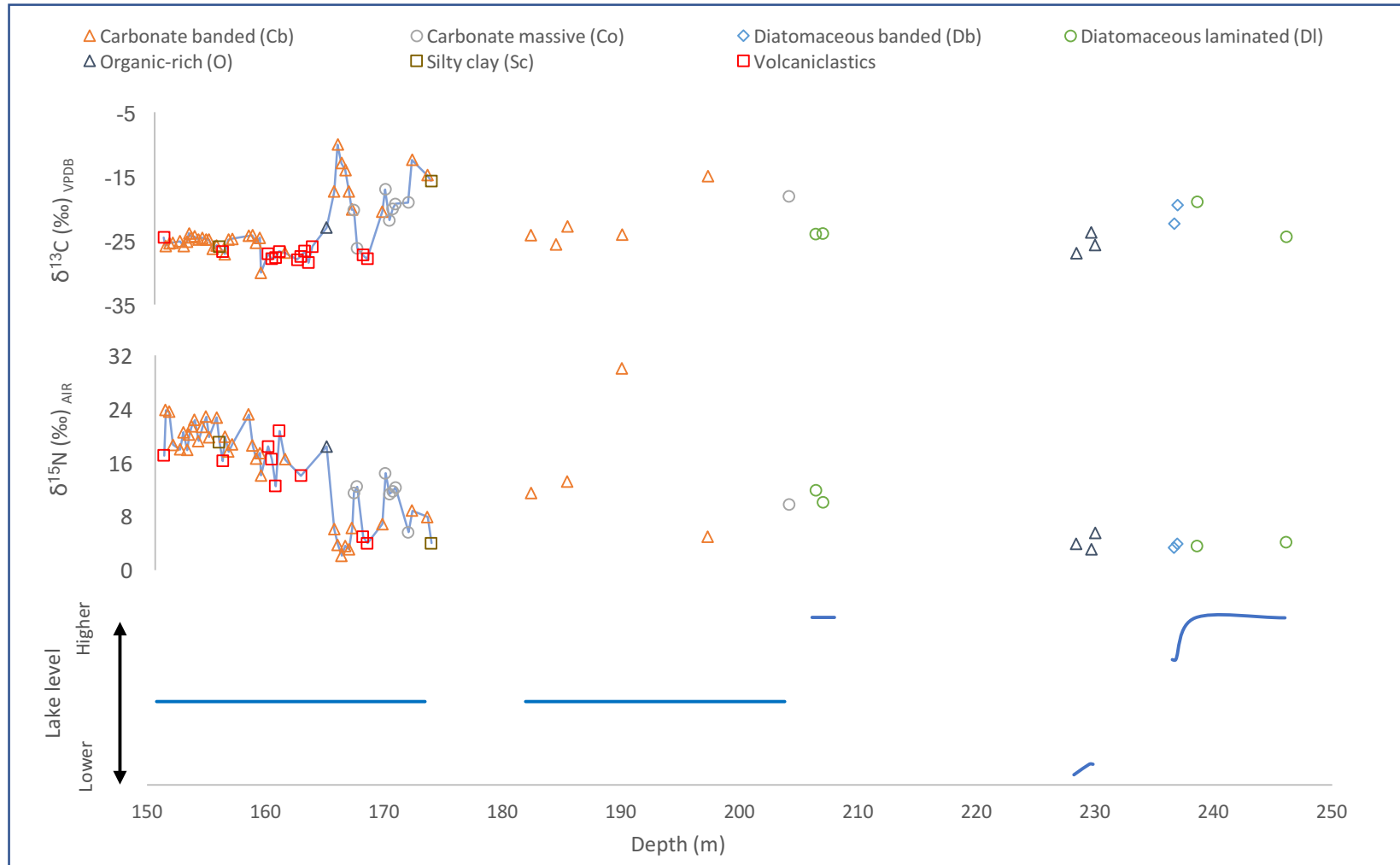


*Figure 14. Carbon and nitrogen isotope ratios of OM in Lake Chalco sediments and interpretation of relative changes in lake water level from depth 246.03-150.77 m.*
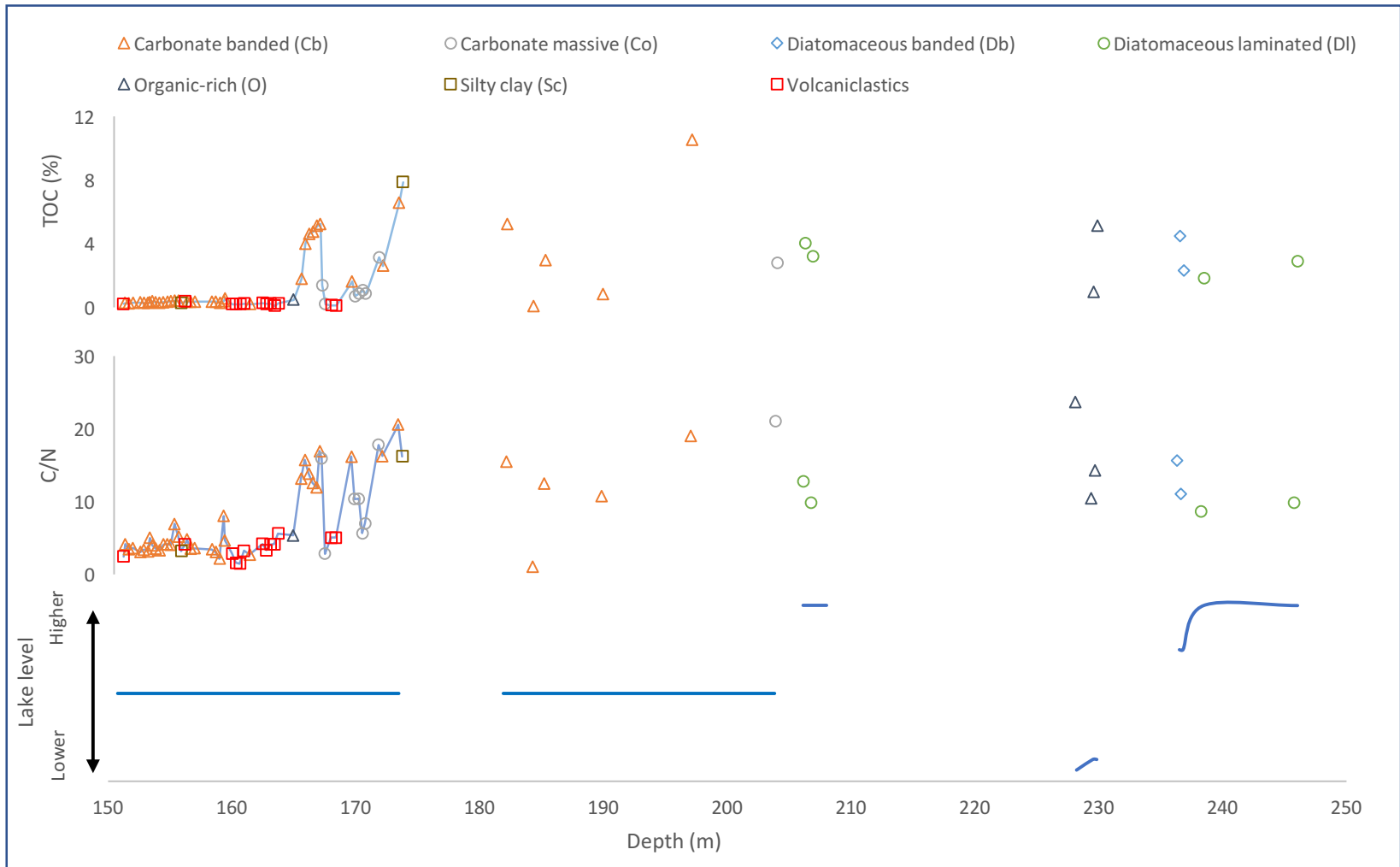
*Figure 15. TOC and C/N results from Lake Chalco organic matter and interpretation of relative changes in lake water level from depth 246.03-150.77 m. TOC for organic-rich sample (35.61%) at 228.20 m not plotted.*
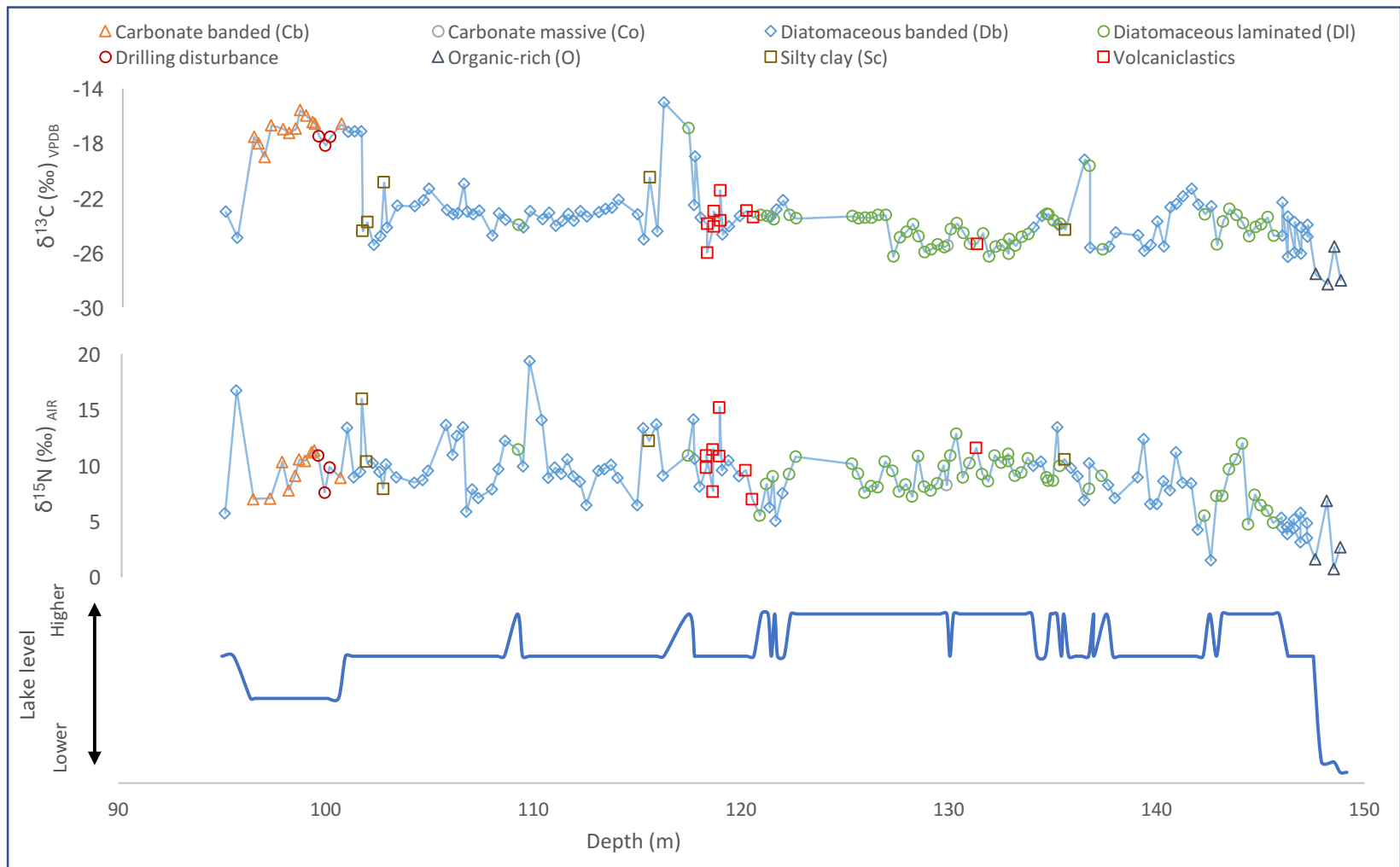
*Figure 16. Carbon and nitrogen isotope ratios of OM in Lake Chalco sediments and interpretations of relative changes in lake water level from depth 149.14-95.01 m.*
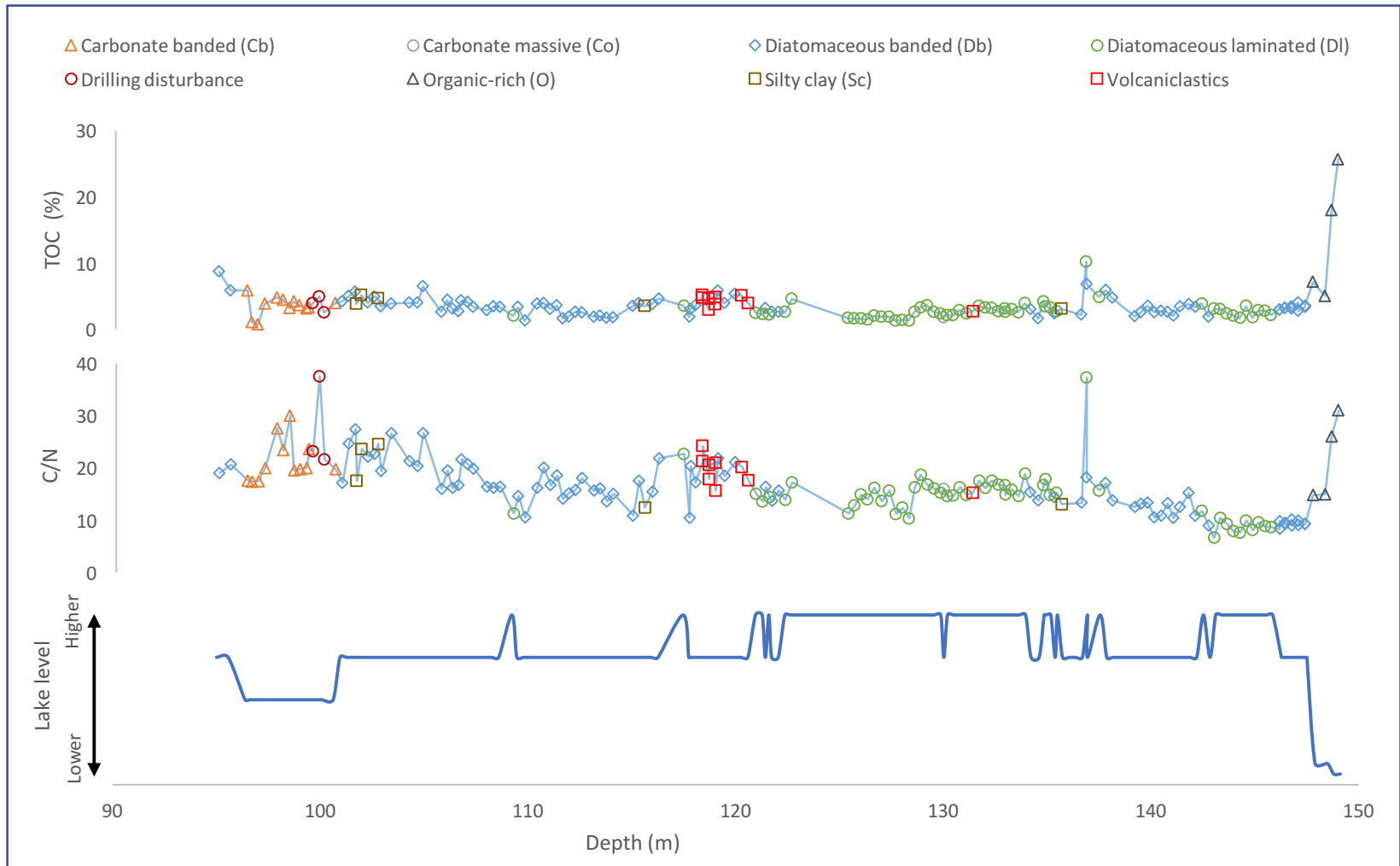
*Figure 17. TOC and C/N results from Lake Chalco organic matter and interpretations of relative changes in lake water level from depth 149.14-95.01 m.*
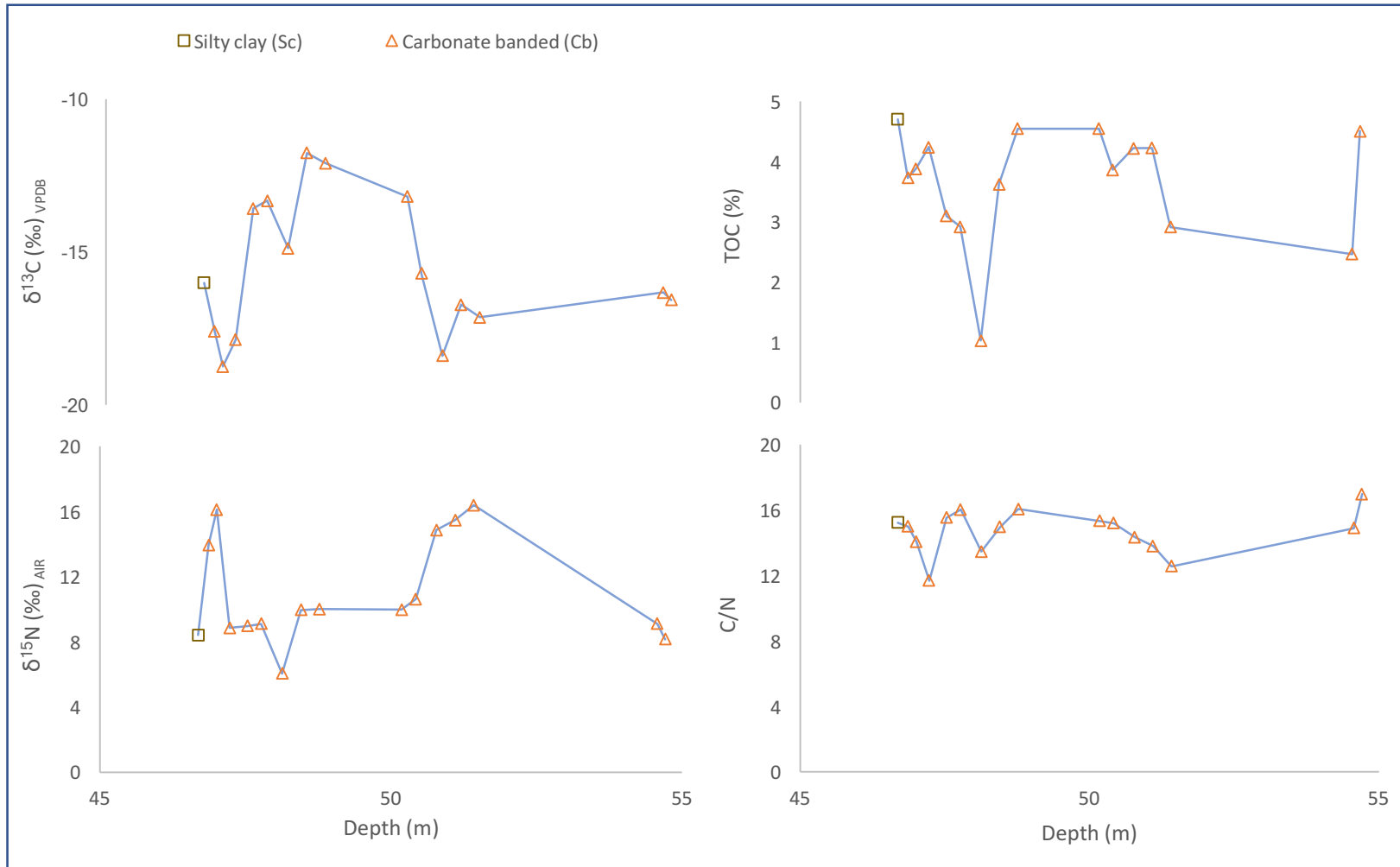
*Figure 18. Carbon and nitrogen isotope ratios of OM, TOC and C/N results from Lake Chalco sediments from depth 54.71-46.37 m. These samples are just below the section of the core that is radiocarbon dated, and are likely in MIS 3.*

**5. Discussion**

**5.1. Interpretations for intervals with numerical age control**

**5.1.1.** *MIS 3 (42-29 ka)*

**5.1.1.i.** *~42-38.6 ka*

The silty clays in this section of the core (mid-MIS 3) (Figure 13) correspond to a deeper lake with higher clastic input and/or lower productivity. The sediments are dominated by silicate minerals with variable diatoms and calcium carbonate minerals (Garcés, B.V. and M. Stockhecke et al., in prep.). Some samples interspersed with the silty clays are identified as volcaniclastic or banded carbonate sediments. All of the samples have higher $\delta^{13}C$ values (-15.10 to -11.04‰). The C/N values of these samples (8.95-18.86) suggest the OM present is dominantly a mixture of algae and macrophytes, possibly with small amounts of C3 plant material. Phytoplankton tissue is richer in nitrogen compared to terrestrial plants, which have higher carbon content due to the construction of cellulose (Talbot and Johannessen, 1992; Meyers and Ishiwatari, 1993; Abbott et al., 2000). As a result, the C/N values for algal OM are generally lower (less than 10-12) than the C/N values for terrestrial vegetation-produced OM (>20) (Talbot and Johannessen, 1992; Meyers and Ishiwatari, 1993; Meyers, 1994; Meyers and Lallier-Vergès, 1999; Abbott et al., 2000; Talbot and Lærdal, 2000). C/N values between 10-20 are generally considered to represent mixing of algal and terrestrial OM (Talbot and Lærdal, 2000). Macrophytes have C/N values that can range from 7.1-29.6 and can contribute significant amounts of OM to lake sediments, particularly in shallow marshy lakes like Chalco (Meyers and Ishiwatari, 1993; Aichner et al., 2010).

The low TOC values (2.00-6.39%) relative to organic-rich lithologies suggest low productivity through this section, so the higher $\delta^{13}C$ values are likely not recording higher productivity. Instead, the higher $\delta^{13}C$ values could be a signal of high pH. The primary control on $\delta^{13}C$ values of organic carbon in autochthonous OM is the $\delta^{13}C$ value of inorganic carbon dissolved in the lake water (Meyers, 1994; Hodell and Schelske, 1998; Abbott et al., 2000; Talbot and Lærdal, 2000). In closed-basin highly evaporative lakes, the pH can become much more basic. Changes in the form of dissolved inorganic carbon from $CO_2$ to $HCO_3^-$ in the hypolimnion at higher pH (>7.4; Stumm and Morgan, 1981) may cause a switch in the photosynthesis pathway employed by plankton, benthic organisms, and macrophytes, and may result in higher $\delta^{13}C$ values (Raven, 1970; Talbot and Johannessen, 1992; Meyers, 2003; Cohen, 2003; Raven et al., 2011).

The nitrogen isotope ratios of OM in these samples are also relatively high (7.08-12.09‰), which could suggest pH is high. At high pH ammonia volatilizes and preferentially releases $^{14}N$ to the atmosphere, generating a strong fractionation (~34‰) that enriches the remaining inorganic nitrogen pool in $^{15}N$ (Talbot and Johannessen, 1992; Talbot and Lærdal, 2000; Cohen, 2003). This can make $\delta^{15}N$ values of OM higher and could be a possible indicator of a more arid climate at this time, or it could the result of volcaniclastics affecting lake pH.

July insolation at 15°N is higher during MIS 3 relative to MIS 2 (Figure 13). However, MIS 3 is not considered a full interglacial period and the ITCZ was likely located further south, keeping precipitation lower at Lake Chalco. Evaporation may have exceeded precipitation during this period, resulting in an alkaline lake and inorganic carbonate precipitation. Indeed, the banded carbonate sediments interspersed in this

section correspond to periods of lower lake level with brackish alkaline water and higher pH. A study by Torres-Rodríguez et al. (2015) found high fire activity at Lake Chalco during MIS 3 that corresponds to a peak in spring insolation. A 2019 study by Caballero et al. of diatoms in a previously-collected Lake Chalco core found that the lake reached hyposaline conditions during MIS 3 (~35 ka) and experienced drought-controlled high frequency lake level oscillations. More information from other proxies, such as diatom species identification or Ti/Ca from scanning XRF, could clarify if the silty clay sediments record a climatic or volcanic signal.

**5.1.1.ii.** *~36-29.2 ka*

The carbonate-rich muds from 36-33.3 ka (Figure 13) correspond to a shallower alkaline brackish lake with higher biogenic productivity. The lower C/N (11.60-19.33) and $\delta^{13}C$ values (-21.00 to -19.55‰) suggest the organic matter is primarily algal with possibly some C3 terrestrial vegetation and macrophyte components (Talbot and Johanessen, 1992; Meyers and Ishiwatari, 1993; Meyers, 1994; Meyers and Lallier-Vergès, 1999; Abbott et al., 2000; Talbot and Lærdal, 2000). The lower $\delta^{13}C$ values suggest the lake is fresher and pH is lower in this section of the core than in the previous section. TOC values (2.52-4.88) are not significantly higher than the silty clays and banded carbonates deposited earlier in MIS 3, suggesting productivity in the lake is relatively low.

Higher $\delta^{15}N$ values (9.98-14.51‰) suggest Lake Chalco was likely seasonally stratified. If the lake is stratified in summer during the primary season of productivity, the hypolimnion often becomes oxygen-depleted or anoxic. The denitrification part of the lake nitrogen cycle takes place in this anoxic water. An increase in the size of the

hypolimnion promotes more denitrification which causes the $\delta^{15}$N OM sediment values to become higher over time (Talbot and Johannessen, 1992; Talbot and Lærdal, 2000; Brandes and Devol, 2002; Meyers, 2003). Increased denitrification in a stratified lake could have resulted in the higher nitrogen isotope values recorded from 36-33.3 ka.

At ~30 ka, the $\delta^{13}$C values in the banded carbonate sediments increase (Figure 13), resembling the results from samples earlier in MIS 3 (~42-38.5 ka). The higher $\delta^{13}$C values (-15.20 to -11.14‰) are likely not a result of high pH or high productivity because $\delta^{15}$N values are much lower (4.67- 5.31‰) than in any previous time in MIS 3. The C/N values of these samples (16.30-17.98) are consistent with a mixture of algal productivity, macrophytes, and C3 vegetation. An increase in macrophyte contribution to OM could explain the higher $\delta^{13}$C values and the lower $\delta^{15}$N values, and is consistent with a shallower lake. The TOC values are higher (7.17-9.73%), supporting the possibility of increased macrophyte abundance during this period. Alternatively, stronger summer stratification could explain the higher $\delta^{13}$C values, as organisms preferentially remove $^{12}$C from the lake epilimnion (Hodell and Schelske, 1998; Talbot and Lærdal, 2000; Leng and Marshall, 2004). Indeed, an explanation for the lower $\delta^{15}$N values is an increase in N-fixing cyanobacteria dominating production in the epilimnion of a stratified Lake Chalco (Talbot and Johannessen,1992; Hodell and Schelske, 1998; Talbot and Lærdal, 2000). In stratified lakes when nitrate becomes a limiting factor, N-fixing cyanobacteria may become dominant in the epilimnion. This can produce lower $\delta^{15}$N values (~0±2‰) that more closely match the $\delta^{15}$N value of the atmosphere (~0.00‰) (Talbot and Johannessen, 1992; Hodell and Schelske, 1998; Talbot and Lærdal; 2000). The banded carbonate muds and likely lake stratification suggest that evaporation exceeded precipitation during this

period. July insolation at 15°N is higher, promoting stronger evaporation. Lake Chalco remained a lower brackish alkaline lake.

The mottled diatomaceous muds present from 29.5-29.2 ka (Figure 13) record a higher lake level than the underlying section. These sediments experienced redox fluctuations that generated mottling during periods of changing stratification regimes. The changing stratification regimes and sediment oxygenation recorded could indicate an unstable climate with changing windiness or periods of reduced summer temperatures that supported year-round mixing. The $\delta^{13}C$ values are lower but still remain relatively high (-16.26 to -15.21‰), possibly suggesting summer stratification driving planktonic organisms to utilize more $^{13}C$ (Hodell and Schelske, 1998; Talbot and Lærdal, 2000; Leng and Marshall, 2004). The C/N values (13.13-15.42) suggest that the primary source of OM is algae or macrophytes. The $\delta^{15}N$ values are higher (7.43-8.38‰) than the values for the underlying carbonate muds, and may be the result of less-persistant stratification and increased utilization of $^{15}N$ by planktonic organisms (Talbot and Johannessen, 1992; Talbot and Lærdal, 2000; Brandes and Devol, 2002; Meyers, 2003).

These sediments are indicative of a deeper lake environment and suggest that precipitation increased in relation to evaporation during this period. A decrease in global temperatures into MIS 2 reduced evaporation, leading to a higher lake level. If annual precipitation remained similar to earlier in MIS 3, but mean annual temperatures decreased, this could alter the hydrologic balance in the catchment by reducing evaporation, and result in a deeper lake.

**5.1.2.** *MIS 2 (29-11.7 ka)*

**5.1.2.i.** *26.5-19 ka: glacial period and Last Glacial Maximum*

The banded diatomaceous muds from 26.5-23.3 ka (Figure 13) record a deeper lake with occasional flood events represented by gray sediments washed in from the watershed or the littoral zone. These samples have periods of both higher (-16.08 to -14.11‰; 26.4-24.9 ka) and lower $\delta^{13}C$ values (-24.17 to -19.92‰; 24.4-23.3 ka). The higher $\delta^{13}C$ values of the earlier samples (26.4-24.9 ka) may record periods of high productivity and summer stratification, resulting in more $^{12}C$ sequestered in the sediments and phytoplankton taking in more $^{13}C$ in the epilimnion (Hodell and Schelske, 1998; Talbot and Lærdal, 2000; Leng and Marshall, 2004). The lower OM $\delta^{13}C$ values of the later samples (24.4-23.3 ka) may correspond to periods of increased mixing that remineralized isotopically-light carbon from the hypolimnion (Cohen, 2003). The C/N values of both groups of banded diatomaceous samples are similar (13.39-17.89) and suggest OM is composed of algal, macrophyte and C3 plant material.

The nitrogen isotope ratios of OM decrease stepwise through this section from ~8‰ to 3.3‰. The reason for this trend is unclear at this time. One possible explanation is increasing amounts of macrophyte and C3 plant material and decreasing amounts of algal material in the lake sediments, suggesting lake level may have been gradually decreasing over this period. The climate was likely cooler with reduced lake evaporation. July insolation at 15°N declined until ~23 ka, reducing evaporation and probably producing lower annual temperatures. Global temperatures were also lower to due reduced atmospheric $CO_2$ (Clark et al., 2009).

The LGM (~22-19 ka) is characterized by organic-rich sediments (Figure 13) that contain sponge spicules, phytoliths, diatoms and terrestrial and amorphous aquatic organic matter (Garcés, B.V. and M. Stockhecke et al., in prep.). These sediments can be peaty or organic-rich silty clays, which suggest a drier, swampy environment rather than a deep lake. Some of the samples from this section have remarkably low $\delta^{13}$C values (-26.91 to -25.31‰). They have the highest TOC (15.21-46.78%) and C/N values (17.83-30.39) in the core analyzed so far. This, combined with the low $\delta^{13}$C values, suggests the primary source of OM is terrestrial C3 plant material (Talbot and Johannessen, 1992; Meyers and Ishiwatari, 1993; Meyers, 1994; Meyers and Lallier-Vergès, 1999; Abbott et al., 2000; Talbot and Lærdal, 2000; Filley et al., 2001; Dawson et al, 2002; Leng and Marshall, 2004; Kohn, 2010). C3 plants use the Calvin-Benson photosynthesis pathway, in which the enzyme ribulose 1,5-biphosphate carboxylase (Rubisco) fixes $CO_2$, resulting in a net discrimination against $^{13}$C of ~27-29‰. This produces organic carbon with $\delta^{13}$C values between -20‰ and -37‰ (Talbot and Johannessen, 1992; Meyers and Ishiwatari, 1993; Meyers, 1994; Filley et al., 2001; Dawson et al., 2002; Leng and Marshall, 2004; Kohn, 2010). In addition, the low $\delta^{15}$N values indicate that there is a significant amount of terrestrial plant material in these samples (~0 ‰). The bulk OM proxies all support the conclusion that these sediments represent a shallow swamp environment.

Lake Chalco appears to have been lower during the LGM, suggesting there was a decrease in precipitation in the Basin of Mexico during this time. Reduced summer precipitation due to low Northern Hemisphere insolation and the southward displacement of the ITCZ likely generated less annual precipitation. However, the swamp environment indicates the water table was relatively high. Cooler temperatures (up to 4°-5°C cooler),

as suggested by Caballero et al. (2019), and reduced evaporation could have supported a swamp environment at Lake Chalco despite reduced precipitation.

The low lake level indicates that winter precipitation did not increase significantly during MIS 2. This suggests the winter storm track, while located further south than the modern position, did not reach far enough south to dramatically increase the number of winter storms in the Basin of Mexico. This contrasts with the recent studies at Peten Itza (e.g. Anselmetti et al., 2006; Hodell et al., 2008; Bush et al., 2009), signifying Chalco and Peten Itza do not necessarily experience the same climate phenomena through the Quaternary.

**5.1.2.ii.** *19-11.7 ka: deglacial*

The organic-rich sediments continue into the deglacial period (~19-11.7 ka) (Figure 13). Some of the results from these organic-rich samples resemble results from similar samples earlier in MIS 2, with high C/N values (23.78-27.12), lower $\delta^{13}$C values (-26.94 to -26.55‰), and lower $\delta^{15}$N values (1.63-1.72‰). These samples record a swampy environment with higher amounts of incoming terrestrial C3 plant OM. However, some organic-rich sediments have lower C/N values (7.13-20.97). They still have lower $\delta^{13}$C values (-26.21 to -18.60‰), but the lower C/N values suggest they contain more algal and/or macrophyte OM. These samples may be from a shallow eutrophic lake environment, rather than a swamp. This suggest that during the deglacial period, Lake Chalco shifted between a largely-terrestrial swamp and a small eutrophic lake. Both environments suggest lake levels remained low during most of the deglacial period.

Two banded diatomaceous samples from the end of MIS 2 (17 ka and 14.9 ka) (Figure 13) suggest a higher lake level. These samples also have the lowest OM $\delta^{15}$N values of any samples analyzed so far. This could be a result of a sudden increase in lake level liberating isotopically-light nitrogen from surrounding soils (e.g. Talbot and Lærdal, 2000). The higher lake level could be the result of melting glaciers on Iztaccihuatl and Popopcatepetl generating more runoff into Lake Chalco as insolation increased into the Holocene (MIS 1).

A sample at ~12.2 ka, within the Young Dryas (~12.8-11.7 ka), is organic-rich (Figure 13). This sample has a much higher $\delta^{13}$C value than the proceeding organic-rich samples, suggesting it may come from a eutrophic lake environment rather than a swamp. The onset of eutrophication can cause the $\delta^{13}$C value to become higher because it speeds up the rate of $^{12}$C removal by photosynthesizing phytoplankton that is then sequestered in the sediment when phytoplankton die (Talbot and Lærdal, 2000; Meyers, 2003). The dissolved inorganic carbon pool in the epilimnion becomes more enriched in $^{13}$C and organic carbon in phytoplankton tissues have higher $\delta^{13}$C values as a result (Hodell and Schelske, 1998; Talbot and Lærdal; 2000; Filley et al., 2001; Meyers, 2003). This suggest lake level decreased again before the Holocene (MIS 1).

### 5.1.3 *MIS 1: early Holocene (11.7-7.5 ka)*

Sampling is sparse through this section. A silty clay sample at 11.2 ka (Figure 13) indicates the lake level increased and clastic deposition overwhelmed OM deposition in the lake sediment. This sample has an unusually high $\delta^{13}$C value (-6.36 ‰), suggesting it may have inorganic carbon contamination. The remaining samples though this section consist of a sample disturbed by drilling (9.40 ka), a volcaniclastic sample (8.56 ka), and

an organic-rich sample (7.55 ka). The organic-rich sample suggests the lake returned to lower levels during the early Holocene. The C/N value (19.98) suggest the OM in this sample is primarily composed of algal and macrophyte material with possibly some C3 plant component. The lower $\delta^{13}C$ value (-24.41‰) and lower $\delta^{15}N$ value (2.89‰) support the conclusion that the sample represents a productive swampy environment. The high July insolation at 15°N at ~11 ka could have led to increased evaporation and a lower lake level. However, the swampy environment suggests the water table was still high or rainfall increased as warmer annual temperatures moved the northern extent of the ITCZ further north during the early Holocene. More sampling could clarify lake level changes during the Holocene.

## 5.2. Interpretations with depth

The samples interpreted by depth are those which are older than the radiocarbon age dating limit (here older than ~42 ka). They are divided into sections using the lithologic classifications of the samples (see Table 1 and Table 2).

### 5.2.1. *246.03-203.82 meters*

The sample interval through the deepest section of the core is sparse, limiting interpretation. Preliminary lithology characterization and bulk OM proxy results suggest there are large fluctuations in lake level between a relatively deep, seasonally-stratified water column and a low-water swampy environment. The deepest samples analyzed are laminated diatomaceous muds (Figure 14). In order to form these sediments, Lake Chalco must have been a fairly deep (~6-8 m water depth; Lewis, 2000) fresh water lake experiencing strong seasonal stratification and hypolimnion anoxia (Garcés, B.V. and M.

Stockhecke et al., in prep.). These samples have lower $\delta^{13}C$ values (~24‰) (Figure 14) and lower C/N values (10-13) (Figure 15), suggesting they contain primarily algal OM.

The next samples analyzed in the section (~228-229 m) are organic-rich (Figure 14) and most likely correspond to a shallow-water swampy or small eutrophic lake environment. They can be peaty, recording the swampy environment, or silty clays that formed in a shallow eutrophic lake. The peaty samples record more C3 terrestrially-dominated OM and the silty clay, eutrophic lake samples record more algal-dominated OM.

The range in OM proxy values for the samples suggests there is variation among these samples and that they likely do not represent the same environment. One of the organic-rich samples has a very high TOC value (~35%) and higher C/N value (~24) (Figure 15) that suggests it contains abundant terrestrial C3 plant material. This sample is likely from a swampy environment. The remaining two organic-rich samples have much lower TOC values (0.96%, 5.12%) and low C/N values (10.49, 14.31) (Figure 15) that suggest they contain mostly algal OM. They may represent a small eutrophic lake environment with high algal productivity, rather than a swampy environment with significant terrestrial C3 input. These organic-rich samples may record an older full glacial period, based on their similarities to LGM samples from MIS 2 (~22-19 kya; core depth 10.3-6 m).

Above this, Lake Chalco returns to higher lake levels, but with sparse sample analysis, the exact depth of this transition in the core is unclear. Diatomaceous banded muds are present at ~237 m depth (Figure 14). The sediment consists of diatomaceous silty clay intercalated with siliciclastic-rich sediments corresponding to a relatively deep

lake dominated by diatom and fine clastic deposition (Garcés, B.V. and M. Stockhecke et al., in prep.). The samples in this section have low C/N (~11-16) (Figure 15) and $\delta^{13}$C values (-19‰ to -22‰) (Figure 14) that suggest OM is dominated by algal production. Samples at ~206 m are laminated diatomaceous muds (Figure 14), suggesting Lake Chalco at this time was deep and experiencing strong seasonal stratification. The C/N values (~8-9) (Figure 15) again suggest OM production is dominated by lacustrine algae. Following this section of core, Lake Chalco appears to transition to a drier environment with enhanced evaporation resulting in the production of calcium carbonate muds.

### 5.2.2. *203.82-150.77 meters*

Sediments in this section are banded or massive carbonate muds and volcaniclastic sediments (Figure 14). The banded carbonate sediments can contain autochthonous calcium carbonate minerals (aragonite or calcite) precipitated from the water column or calcium carbonate formed by organisms, such as ostracods or *Phacotus* (Garcés, B.V. and M. Stockhecke et al., in prep.). They also contain etched diatoms that suggest higher pH (Garcés, B.V. and M. Stockhecke et al., in prep.). The massive carbonates consist of mostly biogenic or autochthonous calcium carbonate laminae. Some are dominated by ostracods or *Phacotus*, and some precipitated directly over volcaniclastic layers (Garcés, B.V. and M. Stockhecke et al., in prep.).

The banded and massive carbonate muds from ~204-165 m (Figure 14) likely represent a relatively shallow alkaline lake with higher evaporation rates. They have a large range in all the OM proxies ($\delta^{13}$C: -26.19 to -10.01‰, TOC: 0.19-10.53%, C/N: 2.86-21.08, $\delta^{15}$N: 2.13-30.04‰) (Figure 14, Figure 15), suggesting there are significantly different lake or watershed conditions within this interval. There is no separation in OM

results between the banded carbonates and massive carbonates in this section. The range in results could record different contributions of algal, macrophyte and C3 plant material in the lake or changes in the strength and duration of summer stratification. The samples with the highest $\delta^{13}C$ values have the lowest $\delta^{15}N$ values. This could record strong summer stratification sequestering $^{12}C$ in the hypolimnion and sediments, and nitrogen fixing cyanobacteria dominating the epilimnion. Alternatively, more abundant macrophytes could generate higher carbon isotope ratios and lower nitrogen isotope rations of OM.

The sediments from ~163-150 m are banded carbonate muds and volcaniclastics (Figure 14). These sediments are unique in the Chalco core because they have unusually high $\delta^{15}N$ values (14.10-23.84‰) (Figure 14) and unusually low TOC values (0.22-0.38%) (Figure 15). Their C/N values are also low (2.16-8.05) (Figure 15) indicating OM in the samples is algal. The low TOC results suggest in-lake productivity was low relative to carbonate sedimentation. The high $\delta^{15}N$ values suggest a higher pH, possibly generating ammonia volatilization. The volcaniclastic sediments consist of tephra, lapilli, pebble to sand-sized sediments of volcanic rock fragments and matrix (Garcés, B.V. and M. Stockhecke et al., in prep.). They are present throughout this section and may have significantly increased lake pH, as well as impacted vegetation in the surrounding watershed. The relative influence of volcanic activity and climate on the samples in this section is difficult to determine at this time, but more inorganic proxies, such as Ti/Ca and oxygen isotopes from carbonates, could help identify changes in watershed erosion and changes in precipitation moisture sources.

### 5.2.3. *150.77-101.59 meters*

The samples from the deepest part of this section (~148 m) are organic-rich muds. These samples have lower $\delta^{13}C$ values (-28.32 to -25.58‰) (Figure 16), high TOC values that decrease upwards (25.63-7.19%) and C/N values that decrease upwards (31-14.83) (Figure 17). The low $\delta^{13}C$ value and the high TOC and C/N values of the first sample suggest it is dominated by C3 terrestrial vegetation OM. This sample likely represents a swampy environment (i.e. low lake level) with high amounts of terrestrial organic matter influx. The younger organic-rich samples in this section have lower TOC and C/N values that suggest they contain more algal OM. These samples may represent a small eutrophic lake that likely formed as Lake Chalco transitioned into a deeper water environment. The organic-rich samples in this section may record an earlier glacial period, similar to what is observed during the LGM in MIS 2 (~22-19 ka; core depth 6-10.3 m).

The sediments that dominate the section of core above the organic-rich sediments are laminated and banded diatomaceous muds (Figure 16). These sediments correspond to a deeper fresher lake experiencing persistent summer stratification (water depth > ~6-8 m; Lewis 2000). C/N (~7-20) (Figure 17) and $\delta^{13}C$ values (-15.04 to -26.34‰) (Figure 16) suggest OM is dominated by algae, possibly with some terrestrial C3 vegetation component. The higher $\delta^{15}N$ values (3.84-19.35‰) (Figure 16) suggest relatively high productivity. The deeper stratified lake indicates more precipitation in the Basin of Mexico and/or it experienced less evaporation. Seasonal stratification indicates warm temperatures during the summer. Lower annual temperatures during a period experiencing strong temperature seasonality could have reduced evaporation, leading to a higher lake level. Further examination of temperature proxies, such as pollen or

biomarkers, could clarify the influence of temperature versus increased precipitation during this period.

### 5.2.4. *101.59-95.01 meters*

In this interval, sediments alternate between banded diatomaceous muds (101-100 m, 95 m) and banded carbonate muds (~96 m) (Figure 16). This suggests variations in in-lake productivity that may be related to periods of fresher and then more alkaline brackish water. The banded diatomaceous muds at the beginning of this section have markedly higher $\delta^{13}$C values (~ -17‰) than the diatomaceous muds in the lower interval (150-102 m) (Figure 16). This may be due to strong seasonal stratification in a warmer environment. Indeed, the banded carbonate muds present in most of this section represent a shallower, more evaporative lake environment likely experiencing higher temperatures. The higher $\delta^{13}$C values (-19.03 to -15.61‰) and $\delta^{15}$N values (7.00-11.36‰) (Figure 16) values of the carbonates suggest a stratified lake with high pH (>7.4; Stumm and Morgan, 1981) in which plankton must use $HCO_3^-$ for photosynthesis. This period was likely drier and warm with reduced precipitation. Significant lake evaporation led to a shallower alkaline lake. The diatomaceous muds sampled just before the gap in the core (~95 m) represent a deeper, fresher lake. The C/N results (19.04 and 20.67) (Figure 17) indicate the OM in these samples is likely mainly algal with possibly some C3 plant OM. This period may have still been warm but increased precipitation could have generated a higher lake level. Without age control at this depth, it is difficult to know how these changes in lake level relate to changing global insolation and glacial-interglacial cycles. The gap in sampling (95.01-54.71 m) in the core occurs after this section.

**5.2.5.** *54.71-46.37 meters*

This section of core is dominated by banded carbonate muds with higher $\delta^{13}C$ values (-18.74 to -11.75‰) and $\delta^{15}N$ values (6.05-16.38‰) (Figure 18). The C/N results (11.68-16.96) (Figure 18) suggest OM is comprised primarily of algal material with a possible contribution from macrophytes and/or C3 plants. The lake is likely shallow and brackish, with periods of stratification during the year. This suggests climate was warmer, with Chalco experiencing strong evaporation and possibly less precipitation.

**6. Conclusions**

We can help answer questions concerning the positions of the ITCZ and the mid-latitude winter jet storm track, and their response to global climate change during the Quaternary using a long core collected from Lake Chalco, Mexico in 2016 by the MexiDrill Project. This study employed bulk organic matter proxies, including total organic carbon, the ratio of total organic carbon/total organic nitrogen, carbon and nitrogen stable isotope ratios of organic matter, and the lithology of samples to investigate changes in lake productivity and hydrology. At this time, age constraints exist for the upper ~42 ka of the core; the remaining older core sections must be interpreted by sections separated by lithology. Results indicate that different lithologies have distinct bulk OM properties.

C/N and $\delta^{13}C$ results indicate most of the banded carbonate sediments likely contain algal and macrophyte-sourced OM, and contain little C3 plant organic matter. These samples likely represent periods of lower lake level during which the lake littoral zone expanded, providing more habitat for macrophytes. The $\delta^{13}C$ and C/N results suggest a mix of algae and C3 plant material dominates the laminated diatomaceous

sediments and a majority of the banded diatomaceous sediments. These samples represent higher lake levels, when the littoral zone likely decreased, reducing macrophyte productivity. The $\delta^{13}C$ and C/N results suggest the organic-rich samples represent either terrestrial swampy environments or a small eutrophic lake.

In the section of the core with age control, changes in lake level appear to correspond to changes in insolation, and most likely the resulting change in the northern position of the ITCZ. During early-mid MIS 3 (~42-30.4 ka), the sediments are silty clays and banded carbonate muds. The silty clays may be the result of watershed disturbance generated by high fire activity or volcanism. The carbonate sediments likely represent warmer, more arid periods with high evaporation and/or less precipitation. As MIS 3 is not a full interglacial period, the ITCZ was likely located further south. Evaporation remained high and Chalco became a shallow alkaline lake.

Later in MIS 3 (~29 ka), the sediments consist of mottled diatomaceous muds that indicate the lake was deeper and experiencing changes in mixing regimes resulting in fluctuations between oxic and anoxic bottom water. These sediments suggest Lake Chalco experienced reduced evaporation. As global temperatures cooled into MIS 2 evaporation from Lake Chalco likely decreased and, in response, lake level rose.

During mid MIS 2 (~26-23.3), the sediments are banded diatomaceous muds, suggesting a deeper lake environment. A cooler climate likely decreased evaporation resulting in a higher lake. The OM proxies suggest the lake was seasonally stratified, with some periods of increased mixing. The LGM (~22-19 ka) consists of organic-rich sediments that likely represent a swampy environment. The bulk proxies suggest C3 vegetation dominates OM in these sediments, supporting their interpretation as a largely-

terrestrial environment. This low lake level suggests reduced precipitation, but the swamp environment indicates cooler temperatures may have reduced evaporation. The northern extent of the ITCZ was located further south during this period, reducing precipitation at Lake Chalco. The winter storm track, deflected south by the Laurentide Ice Sheet during this time, appears to have been located north of Lake Chalco, and winter precipitation did not significantly increase in the Basin of Mexico. The higher water table that supported the swamp environment may be the result of low temperatures and reduced evaporation due to low insolation and global cooling. Banded diatomaceous samples from the end of MIS 2 suggest lake level rose during the transition into the Holocene, possibly as a result of melting glaciers from nearby volcanoes. A sample at ~12.2 ka suggests Chalco was a small eutrophic lake experiencing high algal productivity during the Younger Dryas, just before the Holocene.

Sampling in the Holocene is sparse but lake level appears to remain low. The remaining samples suggest this condition persisted through the early Holocene to 7.55 ka. The bulk OM proxies suggest these organic-rich sediments are from a swampy environment. Higher temperatures may have increased evaporation relative to precipitation, leading to a lower lake level. More sampling through this section could identify lake changes during the early Holocene.
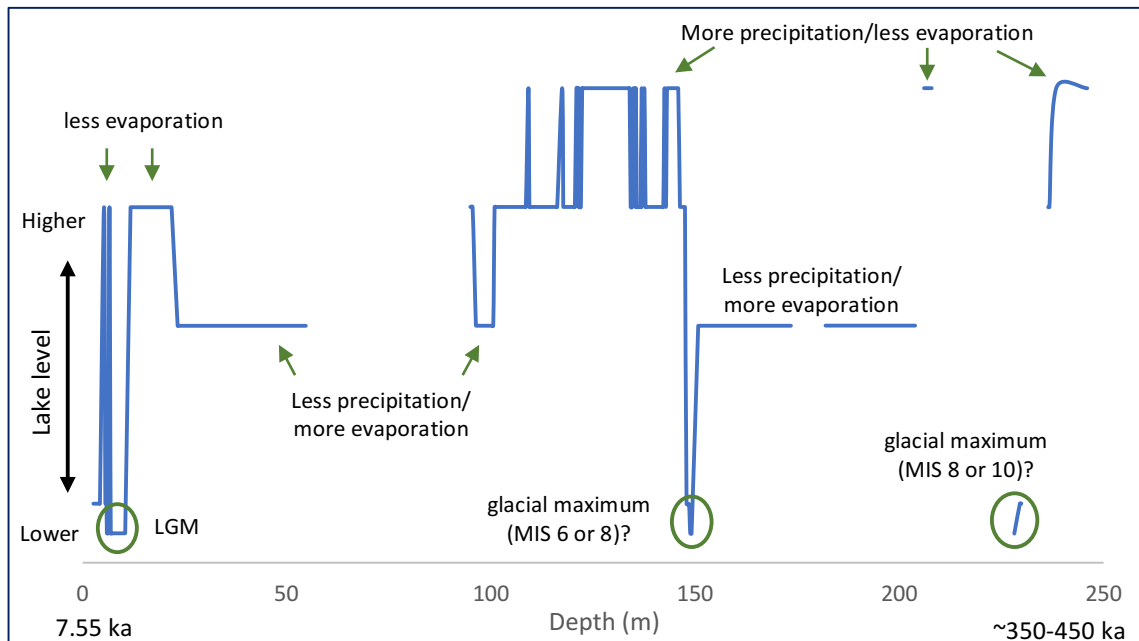
*Figure 19. Interpretation of relative changes in lake water level and corresponding proposed regional climate for the Lake Chalco composite core (2.71-246 m depth). Green circles identify proposed glacial maxima.*

Currently, resolution is poor in the older section of the core analyzed here, but initial results suggest Lake Chalco experienced wetter periods that generated laminated or banded diatomaceous muds and more evaporative periods forming banded or massive carbonate muds. The lowest lake periods correspond to organic-rich sediments that represent a swampy or small eutrophic lake environment. Based on the results from the radiocarbon-dated section of the core, these swamp sediments may record previous glacial maxima during MIS 6, MIS 8, MIS 10 or MIS 12 (Figure 19). Without age control, it is not possible at this time to tie these changes in lake environment to global climate change or glacial-interglacial cycles. However, the sediments and organic matter proxy results suggest Lake Chalco records significant environmental changes related to global insolation and climate change. Understanding natural variability in the ITCZ and winter storm track positions in the neotropics during the Quaternary is crucial to refine

our understanding of how climate may change in the future as a result of anthropogenic

warming.

## References

Abbott, M.B., B.B. Wolfe, R. Aravena, A.P. Wolfe, and G.O. Seltzer (2000), Holocene hydrological reconstructions from stable isotopes and paleolimnology, Cordillera Real, Bolivia, *Quaternary Science Reviews*, 19, 1801-1820.

Aichner, B., U. Herzschuh, and H. Wilkes (2010), Influence of aquatic macrophytes on the stable carbon isotopic signatures of sedimentary organic matter in lakes on the Tibetan Plateau, *Organic Geochemistry*, 41, 706-718.

Amador, J.A., E.J. Alfaro, O.G. Lizano, and V.O. Magaña (2006), Atmospheric forcing of the eastern tropical Pacific: A review, *Progress in Oceanography*, 69, 101-142.

Anselmetti, F.S., D. Ariztegui, D.A. Hodell, M.B. Hillesheim, M. Brenner, A. Gilli, J.A. McKenzie, and A.D. Mueller (2006), Late Quaternary climate-induced lake level variations in Lake Peten Itza, Guatemala, inferred from seismic stratigraphic analysis, *Paleogeography, Palaeoclimatology, Palaeoecology*, 230, 52-69.

Arce, J.L., P.W. Layer, J.C Lassiter, J.A. Benowitz, J.L. Macias, and J. Ramirez-Espinosa (2013), 40Ar/39Ar dating, geochemistry, and isotopic analyses of the quaternary Chichinautzin volcanic field, south of Mexico City: implications for timing, eruption rate, and distribution of volcanism. *Bulletin of Volcanology,* 75, 774.

Berger, A.L. (1992), Orbital variations and insolation database, IGBP PAGES/World Data Center for Paleoclimatology, data contribution series #92-007, NOAA/NGDC Paleoclimatology Program.

Bradbury, J.P. (1971), Paleolimnology of Lake Texcoco, Mexico. Evidence from diatoms, *Limnology and Oceanography*, 16(2), 180-200.

Bradbury, J.P. (1989), Late Quaternary lacustrine paleoenvironments in the Cuenca de Mexico, *Quaternary Science Reviews*, 8, 75-100.

Bradbury, J.P. (1997), Sources of glacial moisture in Mesoamerica, *Quaternary International*, 43/44, 97-110.

Brandes, J.A. and A.H. Devol (2002), A global marine-fixed nitrogen isotopic budget: Implications for Holocene nitrogen cycling, *Global Biogeochemical Cycles*, 26 (4), 1120.

Brenner, M., T.J. Whitmore, J.H. Curtis, D.A. Hodell, and C.L. Schelske (1999), Stable isotope ($\delta^{13}$C and $\delta^{15}$N) signatures of sedimented organic matter as indicators of historic lake trophic state, *Journal of Paleolimnology*, 22, 205-221.

Broccoli, A.J., K.A. Dahl, and R.J. Stouffer (2006), Response of the ITCZ to Northern Hemisphere cooling, *Geophysical Research Letters*, 33, L01702.

Broecker, W.S. (2003), Does the trigger for abrupt climate change reside in the ocean of in the atmosphere? *Science*, 300 (5625), 1519-1522.

Bush, M.B., A.Y. Correa-Metrio, D.A. Hodell, M. Brenner, F.S. Anselmetti, D. Ariztegui, A.D. Mueller, J.H. Curtis, D.A. Grzesik, C. Burton, and A. Gilli (2009), Re-evaluation of climate change in lowland Central America during the Last Glacial Meximum using new sediment cores from Lake Petén Itzá, Guatemala, in F. Vimeux et al. (eds.) *Past Climate Variability in South America and Surrounding Regions*, Developments in Paleoenvironmental Research 14, 113-128.

Caballero-Miranda, M., and B. Ortega-Guerrero (1998), Lake levels since about 40,000 years ago at Lake Chalco, near Mexico City, *Quaternary Research,* 50, 69-79.

Caballero, M., S. Lozano-García, B. Ortega-Guerrero, and A. Correa-Metrio (2019), Quantitative estimates of orbital and millennial scale climatic variability in central Mexico during the last ~40,000 years, *Quaternary Science Reviews*, 205, 62-75.

Caballero-Rodríguez, D., A. Correa-Metrio, S. Lozano-García, S. Sosa-Nájera, B. Ortega, Y. Sanchez-Dzib, K. Aguirre-Navarro, A. Sandoval-Montaño (2018), Late-Quaternary spatiotemporal dynamics of vegetation in Central Mexico, *Review of Palaeobotany and Palynology*, 250, 44-52.

Castañeda, I.S. and S. Schouten (2011), A review of molecular organic proxies for examining modern and ancient lacustrine environments, *Quaternary Science Reviews*, 30, 2851-2891.

Clark, P.U., A.S. Dyke, J.D. Shakun, A.E. Carlson, J. Clark, B. Wohlfarth, J.X. Mitrovica, S.W. Hostetler, A.M. McCabe (2009), The Last Glacial Maximum, *Science*, 325, 710-714.

Clement, A.C., M.A. Cane, and R. Seager (2001), An orbitally driven tropical source for abrupt climate change, *Journal of Climate*, 14 (11), 2369-2375.

Cloern, J.E., E.A. Canuel, and D. Harris (2002), Stable carbon and nitrogen isotope composition of aquatic and terrestrial plants of the San Francisco Bay estuarine system, *Limnology and Oceanography*, 47(3), 713-729.

Cohen, A.S. (2003), Paleolimnology: the history and evolution of lake systems, Oxford University Press, New York, NY, USA.

Cohen, K.M., and P.L. Gibbard (2016), Global chronostratigraphical correlation table for the last 2.7 million years, v. 2016, International Commission on Stratigraphy.

Correa-Metrio, A., S. Lozano-García, S. Xelhuantzi-López, S. Sosa-Nájera, and S.E. Metcalfe (2012), Vegetation in western Central Mexico during the last 50 000 years,

modern analogs and climate in Zacapu Basin, *Journal of Quaternary Science*, 27(5), 509-518.

Correa-Metrio, A., M. Bush, S. Lozano- García, and S. Sosa-Nájera (2013), Millennial-scale temperature change velocity in the continental northern Neotropics, *PLOS One*, 8(12), 1-11.

Dawson, T.E., S. Mambelli, A.H. Plamboeck, P.H. Templer, and K.P. Tu (2002), Stable Isotopes in Plant Ecology, *Annual Review of Ecology and Systematics*, 33, 507-559.

Eadie, B.J., R.L. Chambers, W.S. Gardner, and G.E. Bell (1984), Sediment trap studies in Lake Michigan: Resuspension and chemical fluxes in the southern basin, *Journal of Great Lakes Research*, 10, 307-321.

Froelich, P.N., G.P. Klinkhammer, M.L. Bender, N.A. Luedtke, G.R. Heath, D. Cullen, P. Dauphin, D. Hammond, B. Hartma, V. Maynard (1979), Early oxidation of organic matter in pelagic sediments of the eastern equatorial Atlantic: suboxic diagenesis, *Geochimica et Cosmochimica Acta*, 43(7), 1075-1090.

Escobar, J., D.A. Hodell, M. Brenner, J.H. Curtis, A. Gilli, A.D. Mueller, F.S. Anselmetti, D. Ariztegui, D.A. Grzesik, L. Pérez, A. Schwalb, and T.P. Guilderson (2012), A ~43-ka record of paleoenvironmental change in the Central American lowlands inferred from stable isotopes of lacustrine ostracods, *Quaternary Science Reviews*, 37, 92-104.

Filley, T.R., K.H. Freeman, T.S. Bianchi, M. Baskaran, L.A. Colarusso, and P.G. Hatcher (2001), An isotopic biogeochemical assessment of shifts in organic matter input to Holocene sediments from Mud Lake, Florida, *Organic Geochemistry*, 32, 1153-1167.

Garcés, B.V. and M. Stockhecke et al. (in prep.), Stratigraphy and sedimentology of the Upper Pleistocene-Holocene, Lake Chalco, México Basin, In Limnogeology: Progress, challenges, and opportunities: A tribute to Beth Gierlowski-Kordesch, Ed. M.R. Rosen, L. Park-Bousch, D.B. Finkelstein, S.P. Pueyo, and S. Verlag.

Gibson, K. and L.C. Peterson (2014), A 0.6 million year record of millennial-scale climate variability in the tropics, *Geophysical Research Letters*, American Geophysical Union, 41 (3), 969-975.

Gochis, D.J., C.J. Watts, J. Garatuza-Payan, and J.C. Rodriguez (2007), Spatial and temporal patterns of precipitation intensity as observed by the NAME event rain gauge network from 2002 to 2004, *Journal Climatology,* 20, 1734-1750.

Grauel, A., D.A. Hodell, and S.M. Bernasconi (2016), Quantitative estimates of tropical temperature change in lowland Central America during the last 42 ka, *Earth and Planetary Science Letters*, 438, 37-46.

Harris, D., W.R. Horwáth, and C. van Kessel (2001), Acid fumigation of soils to remove carbonates prior to total organic carbon or carbon-13 isotopic analysis, *Soil Science Society of America Journal*, 65, 1853-1856.

Haug, G.H., K.A. Hughen, D.M. Sigman, L.C. Peterson, and U. Röhl (2001), Southward migration of the Intertropical Convergence Zone through the Holocene, *Science*, 293, 1304-1307.

Herzschuh, U., S. Mischke, H. Meyer, B. Plessen, and C. Zhang (2010), Using variations in the stable isotope composition of macrophyte remains to quantify nutrient dynamics in lakes, *Journal of Paleolimnology*, 43, 739-750.

Hodell, D.A. and Schelske (1998), Production, Sedimentation, and isotopic composition of organic matter in Lake Ontario, *Limnology and Oceanography*, 43(2), 200-214.

Hodell, D.A., F.S. Anselmetti, D. Ariztegui, M. Brenner, J.H. Curtis, A. Gilli, D.A. Grzesik, T. Guilderson, A.D. Muller, M.B. Bush, A. Correa-Metrio, J. Escobar, and S. Kutterolf (2008), An 85-ka record of climate change in lowland Central America, *Quaternary Science Reviews*, 27, 1152-1165.

Holmes, J.A., S.E. Metcalfe, H.L. Jones, and J.D. Marshall (2016), Climatic variability over the last 30 000 years recorded in La Piscina de Yuriria, a Central Mexican crater lake, *Journal of Quaternary Science*, 31(4), 310-324.

Ishiwatari, R. and M. Uzaki (1987), Diagenetic changes of lignin compounds in a more than 0.6 million-year-old lacustrine sediment (Lake Biwa, Japan), *Geochimica et Cosmochimica Acta*, 51(2), 321-328.

Katz, B.J. (1990), Controls on the distribution of lacustrine source rocks through time and space. In Katz, B.J. (Ed.), Lacustrine Basin Exploration: Case Studies and Modern Analogues, American Association of Petroleum Geologists, 61-76.

Keeley, J.E. and D.R. Sandquist (1992), Carbon: freshwater plants, *Plant, Cell, and Environment*, 15, 1021-1035.

Kimmelman, M. (February 17, 2017), Mexico City, parched and sinking, faces a water crisis: climate change is threatening to push a crowded capital toward a breaking point, *The New York Times*, The New York Times Company.

Kohn, M.J. (2010), Carbon isotope compositions of terrestrial C3 plants as indicators of (paleo)ecology and (paleo)climate, *Proceedings of the National Academy of Science*, 107 (46), 19691-19695.

Koutavas, A. and J. Lynch-Stieglitz (2004), Variability of the Marine ITCZ over the eastern Pacific during the past 30,000 years, In: Diaz H.F., Bradley R.S. (eds) The

Hadley Circulation: Present, Past and Future. Advances in Global Change Research, 12. Springer, Dordrecht.

Larson, T.E., J.M. Heikoop, G. Perkins, S.J. Chipera, and M.A. Hess (2008), Pretreatment technique for siderite removal for organic carbon isotope and C:N ratio analysis in geological samples, *Rapid Communications in Mass Spectrometry*, 22, 865-872.

Leng, M.J., and J.D. Marshall (2004), Paleoclimate interpretation of stable isotope data from lake sediment archives, *Quaternary Science Reviews*, 23 (7-8), 811-831.

Leng, M.J., S.E. Metcalfe, and S.J. Davies (2005), Investigating Late Holocene climate variability in central Mexico using carbon isotope ratios in organic materials and oxygen isotope ratios from diatom silica within lacustrine sediments, *Journal of Paleolimnology*, 34, 413-431.

Lin, H., L.C. Peterson, J.T. Overpeck, S.E. Trumbore, and D.W. Murray (1997), Late Quaternary climate change from $\delta^{13}O$ records of multiple species of planktonic foraminifera: High-resolution records from the anoxic Cariaco Basin, Venezuela, *Paleoceanography*, 12 (3), 415-427.

Lisiecki, L.E. and M.E. Raymo (2005), A Pliocene-Pleistocene stack of 57 globally distributed benthid $\delta^{18}O$ records, *Paleoceanography*, 20, PA1003.

Lovan, N.A., and R.V. Krishnamurthy (2000), Late glacial and Holocene paleolimnology of two temperate lakes inferred from sediment organic delta (super 13) C chronology, Proceedings of the Indian Academy of Sciences: Earth and Planetary Sciences, 109 (1), 129-140.

Lozano-García, M.S., B. Ortega-Guerrero, M. Caballero-Miranda, and J. Urrutia-Fucugauchi (1993), Late Pleistocene and Holocene Paleoenvironments of Chalco Lake, Central Mexico, *Quaternary Research*, 40, 332-342.

Lozano-García, S., B. Ortega, P.D. Roy, L. Beramendi-Orosco, and M. Caballero (2015), Climatic Variability in the northern sector of the American tropics since the latest MIS 3, *Quaternary Research*, 84, 262-271.

Lozano-García, S., E.T. Brown, B. Ortega, M. Caballero, J. Werne, P.J. Fawcett, A. Schwalb, B.L. Valero-Garcés, D. Schnurrenberger, R. O'Grady, M. Stockhecke, B. Steinman, E. Cabral-Cano, C. Caballero, S. Sosa-Nájera, A.M. Soler, L. Pérez, A. Noren, A. Myrbo, M. Bücker, N. Wattrus, A. Arciniega, T. Wonik, S. Watt, D. Kumar, C. Acosta, I. Martínez, R. Cossio, T. Ferland, F. Vergara-Huerta (2017), Deep drilling at the Chalco Lake: a technical report, *Boletin de la Sociedad Geological Mexicana*, 69(2), 299-311.

Magrin, G.O., J.A. Marengo, J.P. Boulanger, M.S. Buckeridge, E. Castellanos, G. Poveda, F.R. Scarano, and S. Vicuña (2014), Central and South American, In: Climate Change 2014: Impacts, adaptation, and vulnerability. Part B: Regional aspects, Contribution of Working Group II to the Fifth Assessment Report of the Intergovernmental Panel on Climate Change [Barros, V.R., Field, C.B., Dokken, D.J., Mastrandrea, M.D., Mach, K.J., Bilir, T.E., Chatterjee, M., Ebi, K.L., Estrada, Y.O., Genova, R.C., Girma, B., Kissel, E.S., Levy, A.N., MacCracken, S., Mastrandrea, P.R., and White, L.L. (eds.)], Cambridge University Press, Cambridge, United Kingdom and New York, NY, USA, 1499-1566.

Metcalfe, S.E., S.L. O'Hara, M. Caballero, and S.J. Davies (2000), Records of Late Pleistocene-Holocene climatic change in Mexico—a review, *Quaternary Science Reviews*, 19, 699-721.

Meyers, P.A. (1994), Preservation of elemental and isotopic source identification of sedimentary organic matter, *Chemical Geology*, 114, 289-302.

Meyers, P.A. (2003), Applications of organic geochemistry to paleolimnological reconstructions: a summary of examples from the Laurentian Great Lakes, *Organic Geochemistry*, 34, 261-289.

Meyers, P.A. and E. Lallier-Vergès (1999), Lacustrine sedimentary organic matter records of Late Quaternary paleoclimates, *Journal of Paleolimnology*, 21, 345-372.

Meyers, P.A. and R. Ishiwatari (1993), Lacustrine organic geochemistry—an overview of indicators of organic matter sources and diagenesis in lake sediments, *Organic Geochemistry*, 20(7), 867-900.

Miranda, M.C. (1997), The Last Glacial Maximum in the Basin of Mexico: the diatom record between 34,000 and 15,000 years BP from Lake Chalco, *Quaternary International*, 43/44, 125-136.

Ortega-Guerrero, B., S. Lozano-García, D. Herrera-Hernández, M. Caballero, L. Beramendi-Orosco, J.P. Bernal, E. Torres-Rodríguez, and D. Avendaño-Villeda (2017), Lithostratigraphy and physical properties of lacustrine sediments of the last ca. 150 kyr from Chalco basin, central Mexico, *Journal of South American Earth Sciences*, 79, 507-524.

Ortega-Guerrero, B., and A.J. Newton (1998), Geochemical characterization of Late Pleistocene and Holocene tephra layers from the Basin of Mexico, Central Mexico, *Quaternary Research*, 50, 90-106.

Ortiz-Zamora, D. and A. Ortega-Guerrero (2010), Evolution of long-term land subsidence near Mexico City: reviews, field investigations, and predictive simulations, *Water Resources Research*, 46, W01513.

Ozimek, T. and A. Kowalczewski (1984), Long-term changes of the submerged macrophytes in eutrophic Lake Mikolajskie (North Poland), *Aquatic Botany*, 19, 1-11.

Peterson, L.C., G.H. Haug, K.A. Hughen, and U. Röhl (2000), Rapid changes in the hydrologic cycle of the tropical Atlantic during the last glacial, *Science*, 290, 1947-1951.

Peterson, L.C. and G.H. Haug (2006), Variability in the mean latitude of the Atlantic Intertropical Convergence Zone as recorded by riverine input in sediments to the Cariaco Basin (Venezuela), *Palaeogeography, Palaeoclimatology, Palaeoecology*, 234, 97-113.

Pi, T., S. Lozano-García, M. Caballero-Miranda, B. Ortega-Guerrero, and P. Roy (2010), Discovery and characterization of a struvite layer in the Chalco paleolake, Mexico: *Revista Mexicana de Ciencias Geológicas*, 27 (3), 573–580.

Rasmussen, S.O., M. Bigler, S.P. Blockley, T. Blunier, S.L. Buchardt, H.B. Clausen, I. Cvijanovic, D. Dahl-Jensen, S.J. Johnsen, H. Fischer, V. Gkinis, M. Guillevic, W.Z. Hoek, J.J. Lowe, J.B. Pedro, T. Popp, I.K. Seierstad, J.P. Steffensen, A.M. Svensson, P. Vallelonga, B.M. Vinther, M.J.C. Walker, J.J. Wheatley, M. Winstrup (2014), A stratigraphic framework for abrupt climate changes during the Last Glacial period based on three synchronized Greenland ice-core records: Refining and extending the INTIMATE event stratigraphy, *Quaternary Science Reviews*, 106, 14-28.

Raven, J.A. (1970), Exogenous inorganic carbon source in plant photosynthesis, *Biological Reviews*, 45, 167-221.

Raven, J.A., M. Giordano, J. Beardall, and S.C. Maberly (2011), Algal and aquatic plant carbon concentrating mechanisms in relation to environmental change, *Photosynthesis Research*, 109, 281-296.

Roy, P.D., M. Caballero, R. Lozano, T. Pi, and O. Morton (2009), Late Pleistocene-Holocene geochemical history inferred from Lake Tecocomulco sediments, Basin of Mexico, Mexico, *Geochemical Journal*, 43, 49-64.

Roy, P.D., J.D. Quiroz-Jiménez, L.L. Pérez-Cruz, S. Lozano-García, S.E. Metcalfe, R. Lozano-Santacruz, N. López-Balbiaux, J.L. Sánchez-Zavala, and F.M. Romero (2013), Late Quaternary paleohydrological conditions in the drylands of northern Mexico: a summer precipitation proxy record of the last 80 cal ka BP, *Quaternary Science Reviews*, 78, 342-354.

Rzedowski, G.C. and J. Rzedowski (2001) *Flora fanerogámica del Valle de México*, Instituto de Ecología, A.C. y Comisión Nacional para el Conocimiento y Uso de la Biodiversidad: México.

Sayer, C.D., A. Burgess, K. Kari, T.A. Davidson, S. Peglar, H. Yang, and N. Rose (2010), Long-term dynamics of submerged macrophytes and algae in a small and shallow, eutrophic lake: implications for the stability of macrophyte-dominance, *Freshwater Biology*, 55, 565-583.

Schlegel, I., R. Koschel and L. Krienitz (1998), On the occurrence of *Phacotus lenticularis* (Chlorophyta) in lakes of different trophic state, in *Hydrobiologica*: Phytoplankton and trophic gradients, Eds. M. Alvarez-Cobelas, C.S. Reynolds, P. Sanchez-Castillo and J. Kristiansen, 369/370, 353-361.

Sedov, S., E. Solleiro-Rebolledo, J.E. Gama-Castro, E. Vallejo-Gómez and A. González-Velázquez (2001), Buried palaeosols of the Nevado de Toluca: an alternative record of Late Quaternary environmental change in central Mexico, *Journal of Quaternary Science*, 16(4), 375-389.

Short, D.A. and J.G. Mengel (1986), Tropical climate phase lags and Earth's precession cycle, *Nature*, 323(4), 48-50.

Sigala, I., M. Caballero, A. Correa-Metrio, S. Lozano-García, G. Vázquez, L. Pérez, and E. Zawisza (2017), Basic limnology of 30 continental waterbodies of the Transmexican Volcanic Belt across climatic and environmental gradients, *Boletín de la Sociedad Geológica Mexicana*, 69(2), 313-370.

Solleiro-Rebolledo, E., S. Sedov, E. McClung de Tapia, H. Cabadas, J. Gama-Castro, and E. Vallejo-Gómez (2006), Spatial variability in environmental change in the Teotihuacan Valley during the Lake Quaternary: Paleopedological inferences, *Quaternary International*, 156-157, 13-31.

Solleiro-Rebolledo, E., S. Sycheva, S. Sedov, E. McClung de Tapia, Y. Rivera-Uria, C. Salcido-Berkovich, and A. Kuznetsova (2011), Fluvial processes and paleopedogenesis in the Teotihuacan Valley, México: Responses to late Quaternary environmental change, *Quaternary International*, 233, 40-52.

Stumm, W. and J.J. Morgan (1981), Aquatic chemistry: An introduction emphasizing chemical equilibria in natural waters, second ed, Wiley, New York.

Talbot, M.R. (2001), Nitrogen isotopes in palaeolimnology, In: W.M. Last, J.P Smol (eds), Tracking environmental changes using lake sediments: Physical and chemical techniques, Kluwer, Dordrecht, 401-439.

Talbot, M.R. and T. Johannessen (1992), A high resolution palaeoclimatic record from the last 27,500 years in tropical West Africa from the carbon and nitrogen isotopic composition of lacustrine organic matter, *Earth and Planetary Science Letters*, 110, 23-37.

Talbot, M.R. and T. Lærdal (2000), The Late Pleistocene-Holocene palaeolimnology of Lake Victoria, East Africa based upon elemental and isotopic analyses of sedimentary organic matter, *Journal of Paleolimnology*, 23, 141-164.

Torres-Rodríguez, E., S. Lozano-García, P. Roy, B. Ortega, L. Beramendi-Orosco, A. Correa-Metrio, and M. Caballero (2015), Last Glacial droughts and fire regimes in the central Mexican highlands, *Journal of Quaternary Science*, 30(1), 88-99.

Torres-Rodríguez, E., S. Lozano-García, M. Caballero-Miranda, B. Ortega-Guerrero, S. Sosa-Nájera, and P. Debajyoti-Roy (2018), Pollen and non-pollen palynomorphs of Lake Chalco as indicators of paleolimnological changes in high-elevation tropical central Mexico since MIS 5, *Journal of Quaternary Science*, 1-13.

Vadstrup, M. and T.V. Madsen (1995), Growth limitation of submerged aquatic macrophytes by inorganic carbon, *Freshwater Biology*, 34, 411-419.

van der Hammen, T. (1974), The Pleistocene changes of vegetation and climate in tropical South America, *Journal of Biogeography*, 1(1), 3-26.

Wagner, J.D.M. (2006), Speleothem record of southern Arizona paleoclimate, 54 to 3.5 ka, Department of Geosciences, University of Arizona.

Wagner, J.D.M, J.E. Cole, J.W. Beck, P.J. Patchett, G.M. Henderson, and H.R. Barnett (2010), Moisture variability in the southwestern United States linked to abrupt glacial climate change, *Nature Geoscience*, 3, 110-113.

Watts, W.A. and J.P. Bradbury (1982), Paleoecological studies at Lake Patzcuaro on the West-Central Mexican Plateau and at Chalco in the Basin of Mexico, *Quaternary Research*, 17, 56-60.

# Appendix 1

**Table 2**

| Sample | Splice Depth (m) | Lithology | $\delta^{13}C$ (‰)$_{VPDB}$ | TOC (%) | C/N | $\delta^{15}N$ (‰)$_{AIR}$ |
|---|---|---|---|---|---|---|
| CHA16-1D-1C-1: 31-33 | 2.71 | Organic-rich (O) | -24.41 | 30.54 | 19.98 | 2.89 |
| CHA16-1D-1C-1: 67-70 | 3.07 | Volcaniclastics | -10.65 | 12.89 | 19.05 | 1.92 |
| CHA16-1D-2C-1: 0-3 | 3.36 | Drilling disturbance | -21.85 | 3.97 | 13.84 | 3.30 |
| CHA16-1D-2C-1: 32-35 | 3.68 | Organic-rich (O) | -0.34 | 17.14 | 23.71 | 1.00 |
| CHA16-1D-2C-1: 64-67 | 4.00 | Silty clay (Sc) | -6.36 | 12.33 | 17.40 | 1.77 |
| CHA16-1D-2C-1: 96-99 | 4.32 | Organic-rich (O) | -11.40 | 13.76 | 14.29 | 2.30 |
| CHA16-1D-3C-1: 32-35 | 5.33 | Diatomaceous banded (Db) | -21.22 | 1.41 | 5.70 | -0.22 |
| CHA16-1D-3C-1: 64-67 | 5.65 | Organic-rich (O) | -18.60 | 5.37 | 7.13 | 0.03 |
| CHA16-1D-3C-1: 93-96 | 5.94 | Drilling disturbance | -26.55 | 40.86 | 23.78 | 1.20 |
| CHA16-1D-3C-2: 0-3 | 6.02 | Organic-rich (O) | -26.54 | 45.46 | 25.86 | 1.22 |
| CHA16-1D-3C-2: 32-35 | 6.34 | Organic-rich (O) | -26.94 | 44.21 | 27.12 | 1.29 |
| CHA16-1D-3C-2: 64-67 | 6.66 | Diatomaceous banded (Db) | -18.22 | 15.17 | 16.97 | 0.91 |
| CHA16-1D-3C-2: 96-99 | 6.98 | Organic-rich (O) | -26.21 | 15.21 | 17.83 | 1.28 |
| CHA16-1D-4C-1: 32-35 | 7.44 | Organic-rich (O) | -25.31 | 20.28 | 20.28 | 1.90 |
| CHA16-1D-4C-1: 64-67 | 7.76 | Volcaniclastics | -21.02 | 17.39 | 19.76 | 3.12 |
| CHA16-1D-4C-1: 93-96 | 8.05 | Volcaniclastics | -26.33 | 30.90 | 25.92 | 1.02 |
| CHA16-1D-4C-2: 96-99 | 9.09 | Organic-rich (O) | -26.54 | 29.63 | 25.69 | 2.27 |

**Table 2. Con't**

| Sample | Splice Depth (m) | Lithology | $\delta^{13}C$ (‰)$_{VPDB}$ | TOC (%) | C/N | $\delta^{15}N$ (‰)$_{AIR}$ |
|---|---|---|---|---|---|---|
| CHA16-1D-5C-1: 32-35 | 9.41 | Organic-rich (O) | -26.51 | 38.97 | 30.39 | 1.83 |
| CHA16-1D-5C-2: 8-10 | 10.27 | Organic-rich (O) | -26.21 | 8.86 | 19.18 | 8.06 |
| CHA16-1D-5C-2: 32-35 | 10.51 | Organic-rich (O) | -26.91 | 46.78 | 30.27 | 2.80 |
| CHA16-1D-6C-1: 64-67 | 11.81 | Diatomaceous banded (Db) | -20.36 | 9.48 | 14.67 | 3.27 |
| CHA16-1D-6C-1: 92-95 | 12.09 | Diatomaceous banded (Db) | -19.92 | 5.62 | 13.39 | 5.09 |
| CHA16-1D-6C-2: 64-67 | 12.90 | Diatomaceous banded (Db) | -20.18 | 6.35 | 16.44 | 6.77 |
| CHA16-1D-6C-2: 92-95 | 13.18 | Diatomaceous banded (Db) | -24.17 | 13.88 | 17.86 | 3.77 |
| CHA16-1D-7C-1: 90-93 | 14.02 | Diatomaceous banded (Db) | -15.35 | 5.30 | 15.38 | 6.96 |
| CHA16-1D-7C-2: 3-5 | 14.27 | Diatomaceous banded (Db) | -14.11 | 3.65 | 16.35 | 8.68 |
| CHA16-1D-7C-2: 32-35 | 14.56 | Volcaniclastics | -11.55 | 5.61 | 14.86 | 7.06 |
| CHA16-1D-7C-2: 64-67 | 14.88 | Volcaniclastics | -15.13 | 7.06 | 15.28 | 5.51 |
| CHA16-1D-7C-2: 87-91 | 15.11 | Volcaniclastics | -17.42 | 3.72 | 13.65 | 10.86 |
| CHA16-1D-8C-1: 93-96 | 16.23 | Diatomaceous banded (Db) | -15.76 | 7.13 | 17.68 | 7.42 |
| CHA16-1D-8C-2: 3-5 | 16.44 | Diatomaceous banded (Db) | -16.08 | 7.15 | 16.69 | 6.12 |
| CHA16-1D-8C-2: 32-35 | 16.73 | Volcaniclastics | -15.53 | 3.76 | 15.91 | 11.30 |
| CHA16-1D-10C-2: 32-35 | 21.27 | Diatomaceous mottled (Dm) | -16.26 | 4.84 | 14.34 | 7.43 |
| CHA16-1D-10C-2: 64-67 | 21.59 | Diatomaceous mottled (Dm) | -15.48 | 4.43 | 13.13 | 7.88 |
| CHA16-1D-10C-2: 91-93 | 21.86 | Diatomaceous mottled (Dm) | -15.21 | 3.56 | 15.42 | 8.38 |

**Table 2. Con't**

| Sample | Splice Depth (m) | Lithology | $\delta^{13}C$ (‰)$_{VPDB}$ | TOC (%) | C/N | $\delta^{15}N$ (‰)$_{AIR}$ |
|---|---|---|---|---|---|---|
| CHA16-1D-11C-13: 32-35 | 23.34 | Carbonate banded (Cb) | -11.14 | 9.16 | 17.98 | 5.31 |
| CHA16-1D-11C-13: 64-67 | 23.66 | Carbonate banded (Cb) | -12.48 | 9.73 | 16.66 | 5.12 |
| CHA16-1D-11C-13: 89-92 | 23.91 | Carbonate banded (Cb) | -15.20 | 7.17 | 16.70 | 4.67 |
| CHA16-1A-9Y-1: 96-99 | 28.28 | Carbonate mottled (Cm) | -20.20 | 4.45 | 16.30 | 12.32 |
| CHA16-1A-10Y-1: 0-3 | 28.84 | Carbonate banded (Cb) | -19.95 | 3.98 | 14.48 | 10.18 |
| CHA16-1A-10Y-1: 32-35 | 29.16 | Volcaniclastics | -19.34 | 4.88 | 11.60 | 10.91 |
| CHA16-1A-10Y-1: 64-67 | 29.48 | Carbonate banded (Cb) | -19.82 | 4.38 | 12.80 | 11.58 |
| CHA16-1A-10Y-1: 96-99 | 29.80 | Carbonate banded (Cb) | -20.02 | 3.44 | 16.17 | 11.08 |
| CHA16-1A-10Y-1: 128-131 | 30.12 | Carbonate banded (Cb) | -20.32 | 3.46 | 18.18 | 11.18 |
| CHA16-1A-11Y-1: 0-3 | 30.37 | Carbonate banded (Cb) | -20.36 | 3.48 | 14.77 | 10.04 |
| CHA16-1A-11Y-1: 32-35 | 30.69 | Carbonate banded (Cb) | -21.09 | 2.77 | 17.25 | 12.00 |
| CHA16-1A-11Y-1: 64-67 | 31.01 | Carbonate banded (Cb) | -21.33 | 2.67 | 15.31 | 14.51 |
| CHA16-1A-11Y-1: 96-99 | 31.33 | Carbonate banded (Cb) | -21.36 | 2.56 | 17.14 | 14.31 |
| CHA16-1A-11Y-1: 128-131 | 31.65 | Carbonate banded (Cb) | -21.32 | 2.79 | 17.24 | 11.64 |
| CHA16-1A-12Y-1: 0-3 | 31.89 | Carbonate mottled (Cm) | -21.00 | 2.73 | 15.87 | 11.31 |
| CHA16-1A-12Y-1: 32-35 | 32.21 | Carbonate banded (Cb) | -21.39 | 2.68 | 16.34 | 10.58 |
| CHA16-1A-12Y-1: 64-67 | 32.53 | Carbonate banded (Cb) | -22.36 | 3.11 | 19.33 | 9.98 |

**Table 2. Con't**

| Sample | Splice Depth (m) | Lithology | $\delta^{13}C$ (‰)$_{VPDB}$ | TOC (%) | C/N | $\delta^{15}N$ (‰)$_{AIR}$ |
|---|---|---|---|---|---|---|
| CHA16-1A-12Y-1: 96-99 | 32.85 | Carbonate banded (Cb) | -21.11 | 2.52 | 15.92 | 10.34 |
| CHA16-1A-12Y-1: 128-131 | 33.17 | Carbonate banded (Cb) | -19.55 | 4.31 | 12.02 | 12.03 |
| CHA16-1A-13Y-1: 2-5 | 35.95 | Silty clay (Sc) | -20.66 | 4.81 | 14.25 | 12.55 |
| CHA16-1A-13Y-1: 32-35 | 36.25 | Volcaniclastics | -21.59 | 4.50 | 19.58 | 13.03 |
| CHA16-1A-13Y-1: 64-67 | 36.57 | Volcaniclastics | -19.39 | 7.02 | 17.02 | 11.19 |
| CHA16-1A-13Y-1: 96-99 | 36.89 | Volcaniclastics | -20.20 | 4.21 | 17.22 | 13.99 |
| CHA16-1A-13Y-1: 128-131 | 37.21 | Volcaniclastics | -18.89 | 4.91 | 16.39 | 11.49 |
| CHA16-1A-15Y-1: 32-35 | 39.30 | Silty clay (Sc) | -11.32 | 3.78 | 11.00 | 7.08 |
| CHA16-1A-15Y-1: 64-67 | 39.62 | Silty clay (Sc) | -11.75 | 3.54 | 11.00 | 10.84 |
| CHA16-1C-17Y-1: 0-3 | 39.83 | Silty clay (Sc) | -11.81 | 5.66 | 15.15 | 8.55 |
| CHA16-1A-15Y-1: 96-99 | 39.94 | Silty clay (Sc) | -11.20 | 3.84 | 13.92 | 10.99 |
| CHA16-1C-17Y-1: 28-31 | 40.11 | Silty clay (Sc) | -11.92 | 6.39 | 17.89 | 7.23 |
| CHA16-1A-15Y-1: 128-131 | 40.26 | Carbonate banded (Cb) | -11.94 | 2.87 | 12.63 | 10.56 |
| CHA16-1C-16Y-1: 128-131 | 40.26 | Carbonate banded (Cb) | -11.82 | 2.86 | 12.83 | 9.77 |
| CHA16-1C-17Y-1: 64-67 | 40.47 | Carbonate banded (Cb) | -11.04 | 5.14 | 18.86 | 13.51 |
| CHA16-1C-17Y-1: 96-99 | 40.79 | Carbonate banded (Cb) | -11.63 | 4.39 | 16.91 | 13.26 |
| CHA16-1C-17Y-1: 128-131 | 41.11 | Silty clay (Sc) | -12.48 | 5.08 | 11.96 | 9.55 |
| CHA16-1A-17Y-1: 0-3 | 42.57 | Carbonate banded (Cb) | -12.81 | 6.36 | 15.39 | 10.97 |

**Table 2. Con't**

| Sample | Splice Depth (m) | Lithology | $\delta^{13}C$ (‰)$_{VPDB}$ | TOC (%) | C/N | $\delta^{15}N$ (‰)$_{AIR}$ |
|---|---|---|---|---|---|---|
| CHA16-1A-17Y-1: 28-31 | 42.85 | Silty clay (Sc) | -12.02 | 3.12 | 13.90 | 9.87 |
| CHA16-1A-17Y-1: 64-67 | 43.21 | Volcaniclastics | -12.16 | 5.53 | 16.62 | 9.78 |
| CHA16-1A-17Y-1: 96-99 | 43.53 | Volcaniclastics | -11.47 | 2.62 | 14.43 | 9.00 |
| CHA16-1A-17Y-1: 128-131 | 43.85 | Volcaniclastics | -13.96 | 3.27 | 15.00 | 8.88 |
| CHA16-1A-18Y-1: 4-7 | 44.16 | Silty clay (Sc) | -12.02 | 3.72 | 9.97 | 9.43 |
| CHA16-1A-18Y-1: 28-31 | 44.40 | Silty clay (Sc) | -12.35 | 2.67 | 8.95 | 12.09 |
| CHA16-1A-18Y-1: 64-67 | 44.76 | Silty clay (Sc) | -11.66 | 2.49 | 9.46 | 10.23 |
| CHA16-1A-18Y-1: 96-99 | 45.08 | Silty clay (Sc) | -12.23 | 2.91 | 12.30 | 11.94 |
| CHA16-1A-18Y-1: 128-131 | 45.40 | Silty clay (Sc) | -12.92 | 2.52 | 11.78 | 11.90 |
| CHA16-1A-18Y-1: 150-153 | 45.62 | Silty clay (Sc) | -12.39 | 2.00 | 11.33 | 11.80 |
| CHA16-1A-19Y-1: 4-7 | 45.77 | Carbonate banded (Cb) | -11.04 | 5.60 | 14.29 | 11.07 |
| CHA16-1A-19Y-1: 28-31 | 46.01 | Volcaniclastics | -13.82 | 4.52 | 14.46 | 11.71 |
| CHA16-1A-19Y-1: 64-67 | 46.37 | Silty clay (Sc) | -15.10 | 4.14 | 13.26 | 11.85 |
| CHA16-1A-19Y-1: 96-99 | 46.69 | Silty clay (Sc) | -16.01 | 4.71 | 15.23 | 8.41 |
| CHA16-1A-19Y-1: 114-116 | 46.87 | Carbonate banded (Cb) | -17.59 | 3.73 | 15.00 | 13.93 |
| CHA16-1A-19Y-1: 128-131 | 47.01 | Carbonate banded (Cb) | -18.74 | 3.88 | 14.04 | 16.10 |
| CHA16-1A-19Y-1: 150-153 | 47.23 | Carbonate banded (Cb) | -17.87 | 4.24 | 11.68 | 8.84 |

**Table 2. Con't**

| Sample | Splice Depth (m) | Lithology | $\delta^{13}C$ (‰)$_{VPDB}$ | TOC (%) | C/N | $\delta^{15}N$ (‰)$_{AIR}$ |
|---|---|---|---|---|---|---|
| CHA16-1B-24Y-1: 4-7 | 47.53 | Carbonate banded (Cb) | -13.57 | 3.10 | 15.52 | 8.96 |
| CHA16-1B-24Y-1: 28-31 | 47.77 | Carbonate banded (Cb) | -13.31 | 2.92 | 16.02 | 9.10 |
| CHA16-1B-24Y-1: 64-67 | 48.13 | Carbonate banded (Cb) | -14.87 | 1.03 | 13.46 | 6.05 |
| CHA16-1B-24Y-1: 96-99 | 48.45 | Carbonate banded (Cb) | -11.75 | 3.63 | 14.96 | 9.95 |
| CHA16-1B-24Y-1: 128-131 | 48.77 | Carbonate banded (Cb) | -12.08 | 4.55 | 16.05 | 9.99 |
| CHA16-1B-25Y-1: 4-7 | 50.18 | Carbonate banded (Cb) | -13.18 | 4.55 | 15.33 | 9.97 |
| CHA16-1B-25Y-1: 28-31 | 50.42 | Carbonate banded (Cb) | -15.70 | 3.86 | 15.19 | 10.62 |
| CHA16-1B-25Y-1: 64-67 | 50.78 | Carbonate banded (Cb) | -18.39 | 4.22 | 14.33 | 14.85 |
| CHA16-1B-25Y-1: 96-99 | 51.10 | Carbonate banded (Cb) | -16.71 | 4.23 | 13.79 | 15.45 |
| CHA16-1B-25Y-1: 128-131 | 51.42 | Carbonate banded (Cb) | -17.13 | 2.91 | 12.57 | 16.38 |
| CHA16-1B-27Y-1: 129-131 | 54.57 | Carbonate banded (Cb) | -16.32 | 2.47 | 14.88 | 9.09 |
| CHA16-1B-27Y-1: 143-145 | 54.71 | Carbonate banded (Cb) | -16.56 | 4.51 | 16.96 | 8.15 |
| CHA16-1B-54Y-1: 0-3 | 95.01 | Diatomaceous banded (Db) | -23.04 | 8.72 | 19.04 | 5.71 |
| CHA16-1A-44Y-1: 56-59 | 95.57 | Diatomaceous banded (Db) | -24.92 | 5.91 | 20.67 | 16.73 |
| CHA16-1A-41Y-1: 4-7 | 96.38 | Carbonate banded (Cb) | -17.55 | 5.88 | 17.58 | 7.00 |
| CHA16-1C-50Y-1: 34-37 | 96.59 | Carbonate banded (Cb) | -18.05 | 1.08 | 17.36 | * |
| CHA16-1C-50Y-1: 64-67 | 96.89 | Carbonate banded (Cb) | -19.03 | 0.74 | 17.46 | * |

**Table 2. Con't**

| Sample | Splice Depth (m) | Lithology | $\delta^{13}C$ (‰)$_{VPDB}$ | TOC (%) | C/N | $\delta^{15}N$ (‰)$_{AIR}$ |
|---|---|---|---|---|---|---|
| CHA16-1C-50Y-1: 96-99 | 97.21 | Carbonate banded (Cb) | -16.72 | 3.90 | 20.00 | 7.05 |
| CHA16-1C-51Y-1: 2-5 | 97.80 | Carbonate banded (Cb) | -17.00 | 4.82 | 27.59 | 10.33 |
| CHA16-1C-51Y-1: 32-35 | 98.10 | Carbonate banded (Cb) | -17.26 | 4.49 | 23.36 | 7.78 |
| CHA16-1C-51Y-1: 64-67 | 98.42 | Carbonate banded (Cb) | -16.97 | 3.24 | 30.00 | 9.08 |
| CHA16-1A-42Y-1: 67-70 | 98.61 | Carbonate banded (Cb) | -15.61 | 4.22 | 19.52 | 10.53 |
| CHA16-1A-42Y-1: 96-99 | 98.90 | Carbonate banded (Cb) | -15.99 | 3.68 | 19.76 | 10.43 |
| CHA16-1A-42Y-1: 128-131 | 99.22 | Carbonate banded (Cb) | -16.48 | 3.16 | 19.99 | 11.20 |
| CHA16-1A-42Y-2: 0-3 | 99.34 | Carbonate banded (Cb) | -16.61 | 3.36 | 23.59 | 11.36 |
| CHA16-1A-43Y-1: 0-3 | 99.53 | Drilling disturbance | -17.52 | 3.95 | 23.15 | 10.91 |
| CHA16-1A-43Y-1: 32-35 | 99.85 | Drilling disturbance | -18.19 | 5.01 | 37.52 | 7.58 |
| CHA16-1A-43Y-1: 56-59 | 100.09 | Drilling disturbance | -17.57 | 2.58 | 21.65 | 9.83 |
| CHA16-1B-55Y-1: 32-35 | 100.62 | Carbonate banded (Cb) | -16.61 | 3.97 | 19.77 | 8.90 |
| CHA16-1B-55Y-1: 64-67 | 100.95 | Diatomaceous banded (Db) | -17.21 | 4.23 | 17.18 | 13.38 |
| CHA16-1B-55Y-1: 96-99 | 101.27 | Diatomaceous banded (Db) | -17.17 | 5.05 | 24.67 | 8.92 |
| CHA16-1B-55Y-1: 128-131 | 101.59 | Diatomaceous banded (Db) | -17.17 | 5.72 | 27.38 | 9.42 |
| CHA16-1B-58Y-1: 9-12 | 101.65 | Silty clay (Sc) | -24.43 | 3.89 | 17.53 | 15.97 |
| CHA16-1B-58Y-1: 32-35 | 101.88 | Silty clay (Sc) | -23.79 | 5.18 | 23.62 | 10.37 |
| CHA16-1B-58Y-1: 64-67 | 102.20 | Diatomaceous banded (Db) | -25.44 | 4.05 | 22.17 | 10.23 |

**Table 2. Con't**

| Sample | Splice Depth (m) | Lithology | $\delta^{13}C$ $(‰)_{VPDB}$ | TOC (%) | C/N | $\delta^{15}N$ $(‰)_{AIR}$ |
|---|---|---|---|---|---|---|
| CHA16-1B-58Y-1: 96-99 | 102.52 | Diatomaceous banded (Db) | -24.82 | 5.00 | 22.63 | 9.44 |
| CHA16-1A-46Y-1: 64-67 | 102.68 | Silty clay (Sc) | -20.88 | 4.74 | 24.56 | 7.93 |
| CHA16-1B-58Y-1: 128-131 | 102.84 | Diatomaceous banded (Db) | -24.18 | 3.49 | 19.41 | 10.13 |
| CHA16-1A-46Y-1: 128-131 | 103.32 | Diatomaceous banded (Db) | -22.58 | 3.94 | 26.63 | 8.95 |
| CHA16-1B-59Y-1: 64-67 | 104.20 | Diatomaceous banded (Db) | -22.63 | 4.04 | 21.36 | 8.46 |
| CHA16-1B-59Y-1: 105-108 | 104.61 | Diatomaceous banded (Db) | -22.19 | 4.07 | 20.33 | 8.69 |
| CHA16-1B-59Y-1: 131-134 | 104.87 | Diatomaceous banded (Db) | -21.36 | 6.53 | 26.65 | 9.55 |
| CHA16-1B-60Y-1: 98-101 | 105.75 | Diatomaceous banded (Db) | -22.90 | 2.70 | 16.00 | 13.66 |
| CHA16-1B-60Y-1: 128-131 | 106.05 | Diatomaceous banded (Db) | -23.23 | 4.44 | 19.49 | 10.94 |
| CHA16-1C-56Y-1: 97-100 | 106.28 | Diatomaceous banded (Db) | -23.16 | 3.13 | 16.16 | 12.68 |
| CHA16-1C-56Y-1: 126-129 | 106.57 | Diatomaceous banded (Db) | -21.00 | 2.78 | 16.75 | 13.43 |
| CHA16-1A-48Y-1: 2-5 | 106.72 | Diatomaceous banded (Db) | -23.02 | 4.37 | 21.66 | 5.84 |
| CHA16-1A-48Y-1: 32-35 | 107.02 | Diatomaceous banded (Db) | -23.23 | 4.13 | 20.73 | 7.86 |
| CHA16-1A-48Y-1: 60-63 | 107.30 | Diatomaceous banded (Db) | -22.93 | 3.42 | 19.85 | 7.09 |
| CHA16-1A-49Y-1: 0-3 | 107.96 | Diatomaceous banded (Db) | -24.78 | 2.89 | 16.44 | 7.85 |
| CHA16-1A-49Y-1: 32-35 | 108.28 | Diatomaceous banded (Db) | -23.16 | 3.46 | 16.24 | 9.67 |
| CHA16-1A-49Y-1: 64-67 | 108.60 | Diatomaceous banded (Db) | -23.62 | 3.39 | 16.44 | 12.24 |
| CHA16-1A-49Y-1: 128-131 | 109.24 | Diatomaceous laminated (Dl) | -24.00 | 2.08 | 11.34 | 11.42 |

**Table 2. Con't**

| Sample | Splice Depth (m) | Lithology | $\delta^{13}C$ $(‰)_{VPDB}$ | TOC (%) | C/N | $\delta^{15}N$ $(‰)_{AIR}$ |
|---|---|---|---|---|---|---|
| CHA16-1A-50Y-1: 0-3 | 109.47 | Diatomaceous banded (Db) | -24.19 | 3.38 | 14.68 | 9.93 |
| CHA16-1A-50Y-1: 32-35 | 109.79 | Diatomaceous banded (Db) | -22.99 | 1.33 | 10.53 | 19.35 |
| CHA16-1A-51Y-1: 32-35 | 110.38 | Diatomaceous banded (Db) | -23.58 | 3.88 | 16.19 | 14.10 |
| CHA16-1A-51Y-1: 64-67 | 110.70 | Diatomaceous banded (Db) | -23.09 | 4.02 | 20.09 | 8.87 |
| CHA16-1A-51Y-1: 96-99 | 111.02 | Diatomaceous banded (Db) | -24.05 | 3.09 | 16.70 | 9.80 |
| CHA16-1A-51Y-1: 128-131 | 111.34 | Diatomaceous banded (Db) | -23.72 | 3.62 | 18.57 | 9.24 |
| CHA16-1A-52Y-1: 4-7 | 111.63 | Diatomaceous banded (Db) | -23.19 | 1.72 | 14.08 | 10.53 |
| CHA16-1A-52Y-1: 32-35 | 111.91 | Diatomaceous banded (Db) | -23.71 | 1.97 | 15.16 | 9.01 |
| CHA16-1A-52Y-1: 64-67 | 112.23 | Diatomaceous banded (Db) | -22.98 | 2.63 | 15.81 | 8.55 |
| CHA16-1A-52Y-1: 96-99 | 112.55 | Diatomaceous banded (Db) | -23.40 | 2.61 | 18.04 | 6.45 |
| CHA16-1A-53Y-1: 2-5 | 113.13 | Diatomaceous banded (Db) | -23.06 | 1.94 | 15.66 | 9.54 |
| CHA16-1A-53Y-1: 32-35 | 113.43 | Diatomaceous banded (Db) | -22.83 | 2.08 | 16.10 | 9.69 |
| CHA16-1A-53Y-1: 64-67 | 113.75 | Diatomaceous banded (Db) | -22.74 | 1.73 | 13.63 | 10.05 |
| CHA16-1A-53Y-1: 96-99 | 114.07 | Diatomaceous banded (Db) | -22.15 | 1.83 | 15.08 | 8.90 |
| CHA16-1B-67Y-1: 3-6 | 115.02 | Diatomaceous banded (Db) | -23.22 | 3.56 | 10.91 | 6.44 |
| CHA16-1B-67Y-1: 32-35 | 115.31 | Diatomaceous banded (Db) | -25.04 | 4.01 | 17.56 | 13.36 |
| CHA16-1B-67Y-1: 60-63 | 115.59 | Silty clay (Sc) | -20.53 | 3.54 | 12.47 | 12.20 |
| CHA16-1B-67Y-1: 96-99 | 115.95 | Diatomaceous banded (Db) | -24.47 | 3.84 | 15.51 | 13.70 |

**Table 2. Con't**

| Sample | Splice Depth (m) | Lithology | $\delta^{13}C$ (‰)$_{VPDB}$ | TOC (%) | C/N | $\delta^{15}N$ (‰)$_{AIR}$ |
|---|---|---|---|---|---|---|
| CHA16-1B-67Y-1: 128-131 | 116.27 | Diatomaceous banded (Db) | -15.04 | 4.67 | 21.87 | 9.10 |
| CHA16-1B-68Y-1: 96-99 | 117.48 | Diatomaceous laminated (Dl) | -16.94 | 3.59 | 22.71 | 10.91 |
| CHA16-1C-61Y-1: 2-5 | 117.75 | Diatomaceous banded (Db) | -22.54 | 1.92 | 10.49 | 14.13 |
| CHA16-1B-68Y-1: 128-131 | 117.80 | Diatomaceous banded (Db) | -18.99 | 3.06 | 20.35 | 10.62 |
| CHA16-1C-61Y-1: 32-35 | 118.05 | Diatomaceous banded (Db) | -23.48 | 3.65 | 17.21 | 8.12 |
| CHA16-1A-56Y-1: 64-67 | 118.37 | Volcaniclastics | -23.91 | 4.82 | 21.29 | 9.80 |
| CHA16-1C-61Y-1: 64-67 | 118.37 | Volcaniclastics | -26.00 | 5.22 | 24.20 | 10.90 |
| CHA16-1A-56Y-1: 96-99 | 118.69 | Volcaniclastics | -24.10 | 2.99 | 17.88 | 7.67 |
| CHA16-1C-61Y-1: 96-99 | 118.69 | Volcaniclastics | -22.99 | 4.66 | 20.62 | 11.46 |
| CHA16-1A-56Y-1: 128-131 | 119.01 | Volcaniclastics | -23.66 | 4.89 | 20.96 | 10.86 |
| CHA16-1C-61Y-1: 128-131 | 119.01 | Volcaniclastics | -21.46 | 3.85 | 15.72 | 15.23 |
| CHA16-1B-69Y-1: 96-99 | 119.13 | Diatomaceous banded (Db) | -24.70 | 5.85 | 21.84 | 9.55 |
| CHA16-1B-69Y-1: 128-131 | 119.45 | Diatomaceous banded (Db) | -24.12 | 3.96 | 18.48 | 10.46 |
| CHA16-1A-57Y-1: 64-67 | 119.96 | Diatomaceous banded (Db) | -23.33 | 5.37 | 21.13 | 9.06 |
| CHA16-1A-57Y-1: 96-99 | 120.28 | Volcaniclastics | -22.95 | 5.10 | 20.17 | 9.59 |
| CHA16-1A-57Y-1: 128-131 | 120.60 | Volcaniclastics | -23.43 | 3.99 | 17.63 | 6.98 |
| CHA16-1C-64Y-1: 64-67 | 120.97 | Diatomaceous laminated (Dl) | -23.26 | 2.51 | 15.06 | 5.52 |
| CHA16-1C-64Y-1: 96-99 | 121.29 | Diatomaceous laminated (Dl) | -23.36 | 2.32 | 13.59 | 8.33 |

**Table 2. Con't**

| Sample | Splice Depth (m) | Lithology | $\delta^{13}C$ (‰)$_{VPDB}$ | TOC (%) | C/N | $\delta^{15}N$ (‰)$_{AIR}$ |
|---|---|---|---|---|---|---|
| CHA16-1A-58Y-1: 2-5 | 121.44 | Diatomaceous banded (Db) | -23.41 | 3.25 | 16.38 | 6.23 |
| CHA16-1C-64Y-1: 128-131 | 121.61 | Diatomaceous laminated (Dl) | -23.56 | 2.26 | 14.39 | 9.03 |
| CHA16-1A-58Y-1: 32-35 | 121.74 | Diatomaceous banded (Db) | -22.86 | 2.68 | 13.64 | 5.05 |
| CHA16-1A-58Y-1: 64-67 | 122.06 | Diatomaceous banded (Db) | -22.19 | 2.70 | 15.71 | 7.52 |
| CHA16-1A-58Y-1: 96-99 | 122.38 | Diatomaceous laminated (Dl) | -23.26 | 2.65 | 13.92 | 9.22 |
| CHA16-1A-58Y-1: 128-131 | 122.70 | Diatomaceous laminated (Dl) | -23.50 | 4.63 | 17.24 | 10.80 |
| CHA16-1C-67Y-1: 3-6 | 125.43 | Diatomaceous laminated (Dl) | -23.35 | 1.75 | 11.30 | 10.15 |
| CHA16-1C-67Y-1: 32-35 | 125.72 | Diatomaceous laminated (Dl) | -23.49 | 1.66 | 12.81 | 9.29 |
| CHA16-1C-67Y-1: 64-67 | 126.04 | Diatomaceous laminated (Dl) | -23.45 | 1.65 | 14.89 | 7.58 |
| CHA16-1C-67Y-1: 96-99 | 126.36 | Diatomaceous laminated (Dl) | -23.47 | 1.54 | 14.01 | 8.17 |
| CHA16-1C-67Y-1: 128-131 | 126.68 | Diatomaceous laminated (Dl) | -23.24 | 2.07 | 16.20 | 8.05 |
| CHA16-1C-68Y-1: 4-7 | 127.05 | Diatomaceous laminated (Dl) | -23.27 | 1.95 | 13.67 | 10.34 |
| CHA16-1B-74Y-1: 32-35 | 127.41 | Diatomaceous laminated (Dl) | -26.29 | 1.96 | 15.70 | 9.53 |
| CHA16-1B-74Y-1: 64-67 | 127.73 | Diatomaceous laminated (Dl) | -24.89 | 1.35 | 11.21 | 7.65 |
| CHA16-1B-74Y-1: 96-99 | 128.05 | Diatomaceous laminated (Dl) | -24.49 | 1.46 | 12.40 | 8.31 |
| CHA16-1B-74Y-1: 128-131 | 128.37 | Diatomaceous laminated (Dl) | -23.93 | 1.39 | 10.37 | 7.22 |
| CHA16-1C-70Y-1: 3-6 | 128.64 | Diatomaceous laminated (Dl) | -24.81 | 2.66 | 16.25 | 10.86 |
| CHA16-1C-70Y-1: 32-35 | 128.93 | Diatomaceous laminated (Dl) | -25.97 | 3.36 | 18.72 | 8.11 |

**Table 2. Con't**

| Sample | Splice Depth (m) | Lithology | $\delta^{13}C$ (‰)$_{VPDB}$ | TOC (%) | C/N | $\delta^{15}N$ (‰)$_{AIR}$ |
|---|---|---|---|---|---|---|
| CHA16-1C-70Y-1: 64-67 | 129.25 | Diatomaceous laminated (Dl) | -25.77 | 3.68 | 16.82 | 7.77 |
| CHA16-1C-70Y-1: 96-99 | 129.57 | Diatomaceous laminated (Dl) | -25.43 | 2.71 | 16.12 | 8.42 |
| CHA16-1C-70Y-1: 128-131 | 129.89 | Diatomaceous laminated (Dl) | -25.60 | 2.41 | 15.30 | 9.99 |
| CHA16-1C-70Y-1: 143-145 | 130.04 | Carbonate massive (Co) | -25.49 | 1.86 | 15.97 | 8.25 |
| CHA16-1A-63Y-1: 3-6 | 130.22 | Diatomaceous laminated (Dl) | -24.29 | 2.18 | 14.63 | 10.88 |
| CHA16-1A-63Y-1: 32-35 | 130.51 | Diatomaceous laminated (Dl) | -23.88 | 2.14 | 14.72 | 12.85 |
| CHA16-1A-63Y-1: 64-67 | 130.83 | Diatomaceous laminated (Dl) | -24.56 | 2.92 | 16.30 | 8.92 |
| CHA16-1A-63Y-1: 96-99 | 131.15 | Diatomaceous laminated (Dl) | -25.39 | 2.46 | 14.84 | 10.22 |
| CHA16-1A-63Y-1: 128-131 | 131.47 | Volcaniclastics | -25.37 | 2.77 | 15.30 | 11.57 |
| CHA16-1A-64Y-1: 3-6 | 131.77 | Diatomaceous laminated (Dl) | -24.61 | 3.53 | 17.55 | 9.25 |
| CHA16-1A-64Y-1: 32-35 | 132.06 | Diatomaceous laminated (Dl) | -26.30 | 3.29 | 16.19 | 8.59 |
| CHA16-1A-64Y-1: 64-67 | 132.38 | Diatomaceous laminated (Dl) | -25.59 | 3.23 | 17.58 | 10.90 |
| CHA16-1A-64Y-1: 96-99 | 132.70 | Diatomaceous laminated (Dl) | -25.45 | 2.72 | 16.82 | 10.25 |
| CHA16-1A-64Y-1: 128-131 | 133.02 | Diatomaceous laminated (Dl) | -26.08 | 3.20 | 16.71 | 11.02 |
| CHA16-1C-71Y-1: 32-35 | 133.03 | Diatomaceous laminated (Dl) | -25.00 | 2.64 | 14.91 | 10.40 |
| CHA16-1C-71Y-1: 64-67 | 133.34 | Diatomaceous laminated (Dl) | -25.51 | 3.07 | 15.92 | 9.07 |
| CHA16-1C-71Y-1: 96-99 | 133.66 | Diatomaceous laminated (Dl) | -24.84 | 2.59 | 14.62 | 9.36 |
| CHA16-1C-71Y-1: 128-131 | 133.98 | Diatomaceous laminated (Dl) | -24.68 | 3.95 | 18.89 | 10.65 |

**Table 2. Con't**

| Sample | Splice Depth (m) | Lithology | $\delta^{13}C$ (‰) | TOC (%) | C/N | $\delta^{15}N$ (‰) |
|---|---|---|---|---|---|---|
| CHA16-1C-72Y-1: 1-4 | 134.24 | Diatomaceous banded (Db) | -24.16 | 3.12 | 15.35 | 9.95 |
| CHA16-1C-72Y-1: 40-43 | 134.63 | Diatomaceous banded (Db) | -23.32 | 1.65 | 13.79 | 10.38 |
| CHA16-1C-72Y-1: 64-67 | 134.87 | Diatomaceous laminated (Dl) | -23.20 | 4.27 | 16.75 | 8.93 |
| CHA16-1C-72Y-1: 73-75 | 134.96 | Diatomaceous laminated (Dl) | -23.21 | 3.53 | 17.87 | 8.66 |
| CHA16-1C-72Y-1: 96-99 | 135.19 | Diatomaceous laminated (Dl) | -23.66 | 3.29 | 14.79 | 8.63 |
| CHA16-1A-69Y-1: 65-68 | 135.40 | Diatomaceous banded (Db) | -24.00 | 2.42 | 14.45 | 13.46 |
| CHA16-1C-72Y-1: 128-131 | 135.51 | Diatomaceous laminated (Dl) | -23.90 | 2.75 | 15.26 | 9.99 |
| CHA16-1C-73Y-1: 0-3 | 135.75 | Silty clay (Sc) | -24.34 | 3.15 | 13.11 | 10.56 |
| CHA16-1C-73Y-1: 32-35 | 136.07 | Diatomaceous banded (Db) | * | * | * | 9.77 |
| CHA16-1C-73Y-1: 64-67 | 136.39 | Diatomaceous banded (Db) | * | * | * | 9.02 |
| CHA16-1C-73Y-1: 96-99 | 136.71 | Diatomaceous banded (Db) | -19.22 | 2.22 | 13.35 | 6.88 |
| CHA16-1C-73Y-1: 120-123 | 136.95 | Diatomaceous laminated (Dl) | -19.69 | 10.20 | 37.29 | 7.91 |
| CHA16-1C-74Y-1: 3-6 | 136.96 | Diatomaceous banded (Db) | -25.66 | 6.89 | 18.23 | 10.21 |
| CHA16-1C-74Y-1: 64-67 | 137.57 | Diatomaceous laminated (Dl) | -25.79 | 4.90 | 15.69 | 9.09 |
| CHA16-1C-74Y-1: 96-99 | 137.89 | Diatomaceous banded (Db) | -25.57 | 5.94 | 17.11 | 8.25 |
| CHA16-1C-74Y-1: 128-131 | 138.21 | Diatomaceous banded (Db) | -24.55 | 4.78 | 13.79 | 7.07 |
| CHA16-1A-70Y-1: 2-5 | 139.30 | Diatomaceous banded (Db) | -24.74 | 2.00 | 12.58 | 8.94 |
| CHA16-1A-70Y-1: 32-35 | 139.60 | Diatomaceous banded (Db) | -25.91 | 2.59 | 13.19 | 12.34 |

**Table 2. Con't**

| Sample | Splice Depth (m) | Lithology | $\delta^{13}C$ (‰) | TOC (%) | C/N | $\delta^{15}N$ (‰) |
|---|---|---|---|---|---|---|
| CHA16-1A-70Y-1: 64-67 | 139.92 | Diatomaceous banded (Db) | -25.46 | 3.59 | 13.39 | 6.56 |
| CHA16-1A-70Y-1: 96-99 | 140.24 | Diatomaceous banded (Db) | -23.73 | 2.59 | 10.53 | 6.55 |
| CHA16-1A-70Y-1: 128-131 | 140.56 | Diatomaceous banded (Db) | -25.57 | 2.81 | 10.88 | 8.61 |
| CHA16-1C-77Y-1: 4-7 | 140.88 | Diatomaceous banded (Db) | -22.72 | 2.65 | 13.26 | 7.75 |
| CHA16-1C-77Y-1: 32-35 | 141.16 | Diatomaceous banded (Db) | -22.48 | 2.09 | 10.42 | 11.19 |
| CHA16-1C-77Y-1: 64-67 | 141.48 | Diatomaceous banded (Db) | -21.90 | 3.49 | 12.49 | 8.46 |
| CHA16-1A-72Y-1: 32-35 | 141.90 | Diatomaceous banded (Db) | -21.34 | 3.85 | 15.21 | 8.42 |
| CHA16-1A-72Y-1: 64-67 | 142.22 | Diatomaceous banded (Db) | -22.49 | 3.39 | 10.88 | 4.24 |
| CHA16-1A-72Y-1: 96-99 | 142.54 | Diatomaceous laminated (Dl) | -23.21 | 3.91 | 11.76 | 5.53 |
| CHA16-1A-70Y-1: 128-131 | 140.56 | Diatomaceous banded (Db) | -25.57 | 2.81 | 10.88 | 8.61 |
| CHA16-1A-72Y-1: 128-131 | 142.86 | Diatomaceous banded (Db) | -22.64 | 1.96 | 8.97 | 1.49 |
| CHA16-1C-76Y-1: 3-6 | 143.13 | Diatomaceous laminated (Dl) | -25.42 | 3.15 | 6.65 | 7.26 |
| CHA16-1C-76Y-1: 32-35 | 143.42 | Diatomaceous laminated (Dl) | -23.73 | 3.09 | 10.48 | 7.29 |
| CHA16-1C-76Y-1: 64-67 | 143.74 | Diatomaceous laminated (Dl) | -22.84 | 2.46 | 9.35 | 9.66 |
| CHA16-1C-76Y-1: 96-99 | 144.07 | Diatomaceous laminated (Dl) | -23.25 | 2.12 | 7.92 | 10.58 |
| CHA16-1C-76Y-1: 128-131 | 144.39 | Diatomaceous laminated (Dl) | -23.86 | 1.73 | 7.65 | 12.00 |
| CHA16-1A-74Y-1: 5-8 | 144.68 | Diatomaceous laminated (Dl) | -24.81 | 3.57 | 9.93 | 4.74 |
| CHA16-1A-74Y-1: 37-40 | 145.00 | Diatomaceous laminated (Dl) | -24.14 | 1.83 | 8.10 | 7.38 |

**Table 2. Con't**

| Sample | Splice Depth (m) | Lithology | $\delta^{13}C$ (‰) | TOC (%) | C/N | $\delta^{15}N$ (‰) |
|---|---|---|---|---|---|---|
| CHA16-1A-74Y-1: 64-67 | 145.27 | Diatomaceous laminated (Dl) | -23.95 | 2.91 | 9.60 | 6.44 |
| CHA16-1A-74Y-1: 96-99 | 145.59 | Diatomaceous laminated (Dl) | -23.43 | 2.86 | 8.85 | 5.97 |
| CHA16-1A-74Y-1: 125-128 | 145.88 | Diatomaceous laminated (Dl) | -24.76 | 2.19 | 8.69 | 4.85 |
| CHA16-1A-75Y-1: 5-8 | 146.30 | Diatomaceous banded (Db) | -24.78 | 3.02 | 8.34 | 5.34 |
| CHA16-1C-78Y-1: 5-8 | 146.30 | Diatomaceous banded (Db) | -22.36 | 3.01 | 9.85 | 4.46 |
| CHA16-1A-75Y-1: 32-35 | 146.57 | Diatomaceous banded (Db) | -26.34 | 3.26 | 9.26 | 3.84 |
| CHA16-1C-78Y-1: 32-35 | 146.57 | Diatomaceous banded (Db) | -23.38 | 3.24 | 9.47 | 4.47 |
| CHA16-1A-75Y-1: 64-67 | 146.89 | Diatomaceous banded (Db) | -26.01 | 3.46 | 10.12 | 5.18 |
| CHA16-1C-78Y-1: 64-67 | 146.89 | Diatomaceous banded (Db) | -23.77 | 3.12 | 9.01 | 4.38 |
| CHA16-1A-75Y-1: 96-99 | 147.21 | Diatomaceous banded (Db) | -26.08 | 4.09 | 9.06 | 3.10 |
| CHA16-1C-78Y-1: 96-99 | 147.21 | Diatomaceous banded (Db) | -24.17 | 2.82 | 9.94 | 5.77 |
| CHA16-1A-75Y-1: 128-131 | 147.53 | Diatomaceous banded (Db) | -24.85 | 3.39 | 9.28 | 4.85 |
| CHA16-1C-78Y-1: 128-131 | 147.53 | Diatomaceous banded (Db) | -24.00 | 3.60 | 9.33 | 3.51 |
| CHA16-1A-76Y-1: 6-9 | 147.92 | Organic-rich (O) | -27.59 | 7.19 | 14.83 | 1.58 |
| CHA16-1A-76Y-1: 64-67 | 148.50 | Organic-rich (O) | -28.32 | 5.10 | 14.96 | 6.81 |
| CHA16-1A-76Y-1: 96-99 | 148.82 | Organic-rich (O) | -25.58 | 17.94 | 26.02 | 0.72 |
| CHA16-1A-76Y-1: 128-131 | 149.14 | Organic-rich (O) | -28.04 | 25.63 | 31.00 | 2.67 |
| CHA16-1A-77Y-1: 128-131 | 150.77 | Volcaniclastics | -24.52 | 0.20 | 2.46 | 17.08 |

**Table 2. Con't**

| Sample | Splice Depth (m) | Lithology | $\delta^{13}C$ (‰) | TOC (%) | C/N | $\delta^{15}N$ (‰) |
|---|---|---|---|---|---|---|
| CHA16-1B-88Y-1: 32-35 | 150.90 | Carbonate banded (Cb) | -25.83 | 0.26 | 4.17 | 23.84 |
| CHA16-1B-88Y-1: 64-67 | 151.22 | Carbonate banded (Cb) | -25.43 | 0.22 | 3.44 | 23.59 |
| CHA16-1B-88Y-1: 96-99 | 151.54 | Carbonate banded (Cb) | -25.34 | 0.27 | 3.64 | 18.64 |
| CHA16-1B-89Y-1: 3-6 | 152.13 | Carbonate banded (Cb) | -25.11 | 0.29 | 3.07 | 17.96 |
| CHA16-1B-89Y-1: 32-35 | 152.42 | Carbonate banded (Cb) | -25.84 | 0.25 | 3.39 | 20.52 |
| CHA16-1B-89Y-1: 64-67 | 152.74 | Carbonate banded (Cb) | -25.17 | 0.26 | 3.18 | 17.89 |
| CHA16-1A-78Y-1: 53-56 | 152.90 | Carbonate banded (Cb) | -23.86 | 0.30 | 5.03 | 20.15 |
| CHA16-1A-79Y-1: 5-8 | 153.10 | Carbonate banded (Cb) | -24.49 | 0.37 | 4.01 | 21.40 |
| CHA16-1A-79Y-1: 32-35 | 153.37 | Carbonate banded (Cb) | -24.35 | 0.31 | 3.58 | 22.38 |
| CHA16-1A-79Y-1: 64-67 | 153.69 | Carbonate banded (Cb) | -24.81 | 0.27 | 3.35 | 19.25 |
| CHA16-1A-79Y-1: 96-99 | 154.01 | Carbonate banded (Cb) | -24.56 | 0.31 | 4.14 | 21.31 |
| CHA16-1A-80Y-1: 5-8 | 154.33 | Carbonate banded (Cb) | -24.83 | 0.35 | 4.15 | 22.85 |
| CHA16-1A-80Y-1: 32-35 | 154.60 | Carbonate banded (Cb) | -24.85 | 0.36 | 4.07 | 19.78 |
| CHA16-1A-80Y-1: 64-67 | 154.92 | Carbonate banded (Cb) | -26.32 | 0.39 | 6.95 | * |
| CHA16-1A-80Y-1: 96-99 | 155.24 | Carbonate banded (Cb) | -25.74 | 0.40 | 5.19 | 22.75 |
| CHA16-1A-80Y-1: 118-121 | 155.46 | Silty clay (Sc) | -25.95 | 0.27 | 3.23 | 19.08 |
| CHA16-1A-80Y-2: 0-3 | 155.75 | Volcaniclastics | -26.71 | 0.36 | 4.11 | 16.27 |
| CHA16-1A-81Y-1: 3-6 | 155.94 | Carbonate banded (Cb) | -27.13 | 0.34 | 4.81 | 19.89 |

**Table 2. Con't**

| Sample | Splice Depth (m) | Lithology | $\delta^{13}C$ (‰) | TOC (%) | C/N | $\delta^{15}N$ (‰) |
|---|---|---|---|---|---|---|
| CHA16-1A-81Y-1: 32-35 | 156.23 | Carbonate banded (Cb) | -24.85 | 0.32 | 3.51 | 17.63 |
| CHA16-1A-81Y-1: 64-67 | 156.55 | Carbonate banded (Cb) | -24.72 | 0.34 | 3.60 | 18.71 |
| CHA16-1C-88Y-1: 32-35 | 157.95 | Carbonate banded (Cb) | -24.26 | 0.34 | 3.47 | 23.20 |
| CHA16-1C-88Y-1: 64-67 | 158.27 | Carbonate banded (Cb) | -24.19 | 0.35 | 3.09 | 18.53 |
| CHA16-1C-88Y-1: 96-99 | 158.59 | Carbonate banded (Cb) | -25.31 | 0.28 | 2.16 | 16.61 |
| CHA16-1C-88Y-1: 128-131 | 158.91 | Carbonate banded (Cb) | -24.56 | 0.38 | 8.05 | 17.44 |
| CHA16-1B-92Y-1: 64-67 | 159.00 | Carbonate banded (Cb) | -30.03 | 0.54 | 4.70 | 14.10 |
| CHA16-1C-89Y-1: 32-35 | 159.60 | Volcaniclastics | -27.09 | 0.18 | 2.89 | 18.42 |
| CHA16-1C-89Y-1: 64-67 | 159.92 | Volcaniclastics | -27.84 | 0.18 | 1.61 | 16.51 |
| CHA16-1C-89Y-1: 96-99 | 160.24 | Volcaniclastics | -27.69 | 0.19 | 1.50 | 12.52 |
| CHA16-1C-89Y-1: 128-131 | 160.56 | Volcaniclastics | -26.70 | 0.22 | 3.26 | 20.74 |
| CHA16-1A-86Y-1: 15-18 | 161.03 | Carbonate banded (Cb) | -26.92 | 0.18 | 2.72 | 16.51 |
| CHA16-1C-90Y-1: 0-3 | 162.07 | Volcaniclastics | -27.99 | 0.26 | 4.20 | * |
| CHA16-1C-90Y-1: 32-35 | 162.39 | Volcaniclastics | -27.47 | 0.20 | 3.34 | 14.05 |
| CHA16-1C-90Y-1: 64-67 | 162.71 | Volcaniclastics | -26.66 | 0.22 | 4.12 | * |
| CHA16-1C-90Y-1: 96-99 | 163.03 | Volcaniclastics | -28.43 | 0.09 | 4.18 | * |
| CHA16-1C-90Y-1: 128-131 | 163.35 | Volcaniclastics | -25.94 | 0.24 | 5.62 | * |
| CHA16-1C-91Y-1: 96-99 | 164.58 | Organic-rich (O) | -23.00 | 0.46 | 5.36 | 18.40 |

**Table 2. Con't**

| Sample | Splice Depth (m) | Lithology | $\delta^{13}C$ (‰) | TOC (%) | C/N | $\delta^{15}N$ (‰) |
|---|---|---|---|---|---|---|
| CHA16-1C-92Y-1: 2-5 | 165.22 | Carbonate banded (Cb) | -17.37 | 1.77 | 13.14 | 6.06 |
| CHA16-1C-92Y-1: 32-35 | 165.52 | Carbonate banded (Cb) | -10.01 | 3.97 | 15.76 | 3.69 |
| CHA16-1C-92Y-1: 64-67 | 165.84 | Carbonate banded (Cb) | -12.91 | 4.62 | 13.85 | 2.13 |
| CHA16-1C-92Y-1: 96-99 | 166.16 | Carbonate banded (Cb) | -14.00 | 4.76 | 12.59 | 3.56 |
| CHA16-1C-92Y-1: 128-131 | 166.48 | Carbonate banded (Cb) | -17.37 | 5.11 | 11.96 | 3.11 |
| CHA16-1A-90Y-1: 17-20 | 166.74 | Carbonate banded (Cb) | -20.15 | 5.22 | 16.93 | 6.26 |
| CHA16-1C-93Y-1: 6-9 | 166.90 | Carbonate massive (Co) | -20.23 | 1.37 | 15.96 | 11.48 |
| CHA16-1C-93Y-1: 32-35 | 167.16 | Carbonate massive (Co) | -26.19 | 0.19 | 2.86 | 12.41 |
| CHA16-1C-93Y-1: 82-85 | 167.66 | Volcaniclastics | -27.26 | 0.12 | 5.05 | 4.93 |
| CHA16-1C-93Y-1: 120-123 | 168.04 | Volcaniclastics | -27.85 | 0.11 | 5.08 | 4.01 |
| CHA16-1C-94Y-1: 96-99 | 169.31 | Carbonate banded (Cb) | -20.45 | 1.61 | 16.20 | 6.83 |
| CHA16-1C-94Y-1: 121-124 | 169.56 | Carbonate massive (Co) | -17.02 | 0.68 | 10.37 | 14.41 |
| CHA16-1C-95Y-1: 3-6 | 169.90 | Carbonate massive (Co) | -21.85 | 0.86 | 10.42 | 11.34 |
| CHA16-1C-95Y-1: 32-35 | 170.19 | Carbonate massive (Co) | -20.04 | 1.04 | 5.65 | 11.74 |
| CHA16-1C-95Y-1: 55-57 | 170.42 | Carbonate massive (Co) | -19.26 | 0.85 | 7.04 | 12.31 |
| CHA16-1A-94Y-1: 32-35 | 171.51 | Carbonate massive (Co) | -19.07 | 3.13 | 17.81 | 5.63 |
| CHA16-1A-94Y-1: 64-67 | 171.83 | Carbonate banded (Cb) | -12.39 | 2.61 | 16.28 | 8.86 |
| MEXI-CHA16-1A-95Y-1 | 173.13 | Carbonate banded (Cb) | -14.80 | 6.58 | 20.61 | 7.91 |

**Table 2. Con't**

| Sample | Splice Depth (m) | Lithology | δ¹³C (‰) | TOC (%) | C/N | δ¹⁵N (‰) |
|---|---|---|---|---|---|---|
| CHA16-1A-95Y-1: 64-67 | 173.45 | Silty clay (Sc) | -15.69 | 7.86 | 16.23 | 3.98 |
| CHA16-1C-100Y-1: 96-99 | 181.917 | Carbonate banded (Cb) | -24.11 | 5.21 | 15.51 | 11.44 |
| CHA16-1A-102Y-1: 2-5 | 184.061 | Carbonate banded (Cb) | -25.59 | 0.04 | 1.06 | * |
| CHA16-1A-102Y-1: 96-99 | 185.001 | Carbonate banded (Cb) | -22.78 | 2.97 | 12.50 | 13.22 |
| CHA16-1A-105Y-1: 96-99 | 189.662 | Carbonate banded (Cb) | -24.06 | 0.83 | 10.74 | 30.04 |
| CHA16-1C-109Y-1: 96-99 | 196.935 | Carbonate banded (Cb) | -14.93 | 10.53 | 19.06 | 4.93 |
| CHA16-1C-113Y-1: 128-131 | 203.819 | Carbonate massive (Co) | -18.08 | 2.76 | 21.08 | 9.79 |
| CHA16-1A-116Y-1: 64-67 | 206.099 | Diatomaceous laminated (Dl) | -23.97 | 4.03 | 12.79 | 11.88 |
| CHA16-1C-115Y-1: 96-99 | 206.709 | Diatomaceous laminated (Dl) | -23.93 | 3.21 | 9.86 | 10.05 |
| CHA16-1C-129Y-1: 64-67 | 228.201 | Organic-rich (O) | -27.01 | 35.61 | 23.68 | 3.87 |
| CHA16-1A-135Y-1: 32-35 | 229.496 | Organic-rich (O) | -23.77 | 0.96 | 10.49 | 3.07 |
| CHA16-1A-135Y-1: 64-67 | 229.816 | Organic-rich (O) | -25.71 | 5.12 | 14.31 | 5.52 |
| CHA16-1B-140Y-1: 120-123 | 236.511 | Diatomaceous banded (Db) | -22.37 | 4.48 | 15.68 | 3.34 |
| CHA16-1C-134Y-1: 32-35 | 236.801 | Diatomaceous banded (Db) | -19.48 | 2.29 | 11.06 | 3.87 |
| CHA16-1C-135Y-1: 64-67 | 238.456 | Diatomaceous laminated (Dl) | -18.96 | 1.83 | 8.69 | 3.54 |
| CHA16-1C-140Y-1: 64-67 | 246.027 | Diatomaceous laminated (Dl) | -24.42 | 2.87 | 9.83 | 4.11 |

* Measured amplitude too low to generate accurate results.